Thesis for the Degree of Master of Science

Structure and Phase Transition in Thin Films of Semifluorinated Block Copolymer Micelles Complexed with Gold Precursor

by

Nguyen Thi Hoai An

Department of Image Science and Engineering

The Graduate School

Pukyong National University

August 2011

Structure and Phase Transition in Thin Films of Semifluorinated Block Copolymer Micelles Complexed with Gold Precursor

(금전구체와 혼합된 부분불소화 블록 공중합체 마이셀 박막 필름 구조 및 상전이에 대한 연구)

Advisor: Prof. Kwon Taek Lim

By

Nguyen Thi Hoai An

A thesis submitted in partial fulfillment of the requirements

for the degree of

Master of Science

in Department of Image Science and Engineering, The Graduate School,

Pukyong National University

August 2011

Structure and Phase Transition in Thin Films of Semifluorinated Block copolymer Micelles Complexed with Gold Precursor

A dissertation

by

Nguyen Thi Hoai An

Approved by:

Jong Tae Kim, Ph.D. (Chairman)

Yeon Tae Jeong, Ph.D. (Member)

Kwon Taek Lim, Ph.D. (Member)

August 2011

Dedicated to My Loving Parents

Nguyen Dang Hiep

And

Le Thi Ngoc Nga

Structure and Phase Transition in Thin Films of Semifluorinated Block Copolymer Micelles Complexed with Gold Precursor

Nguyen Thi Hoai An

Department of Image Science and Engineering, the Graduate School, Pukyong National University

Abstract

An approach for preparing the ordered structures of Au/polymer nanocomposites is discussed, which employs solvent vapor, supercritical CO_2 and thermal annealing process for Au-loaded poly(1H,1H-dihydroperfluorooctyl methacrylate)-*b*-poly(ethylene oxide) (PFOMA-*b*-PEO) and Au-loaded poly(3-hexylthiophene)-b-poly(1H,1H-dihydroperfluorooctyl methacrylate) (P3HT-b-PFOMA) thin films. Semifluorinated diblock copolymers $PFOMA_{10k}$-*b*-EO_{12k} was prepared by atom transfer radical polymerization (ATRP), and its micellar solution with a gold precursor, $LiAuCl_4$, in chloroform was spin-coated onto substrate to produce thin hybrid films. After annealing, the chains were reorganized and formed spherical copolymeric films. The nanoparticles were forced to follow the morphological change and were transformed into a larger single particle in each PEO domain. In the case of $P3HT_{4k}$-b-$PFOMA_{14k}$, the block copolymers underwent microphase separation and self-assembly into well-defined and organized nanofibrillar-like morphology from their micelle solution. The gold nanoparticles were stabilized by the interaction of the sulfur atoms of P3HTs with the gold surface and they dispersed in the P3HT phase. The length of nanofibrils increased a little with pronounced branching after thermal annealing, solvent annealing and $scCO_2$ annealing in the micellar films with the Au nanoparticles.

금전구체와 혼합된 부분불소화 블록 공중합체 마이셀 박막 필름 구조 및 상전이에 대한 연구

응웬 티 호아이 안

부경대학교 대학원 이미지시스템공학과

요약

잘 배열된 Au/polymer 나노 합성을 위한 접근법들이 논의되었다. 이것은 솔벤트 베이퍼, 초임계 이산화탄소, thermal annealing 과정이 이용되는데 이것은 Au-loaded poly(1H,1H-dihydroperfluorooctyl methacrylate)-*b*-poly(ethylene oxide) (PFOMA-*b*-PEO) 와 Au-loaded poly(3-hexylthiophene)-b-poly(1H,1H-dihydroperfluorooctyl methacrylate) (P3HT-b-PFOMA) thin films 를 만들기 위함입니다. 혼합된 부분불소화 블록 공중합체 다이블록 공중합체 $PFOMA_{10k}$-*b*-EO_{12k} 는 원자전이 라디칼중합(ATRP)에 의해서 준비되었다. 그리고 클로로포름에 녹아있는 금전구체, $LiAuCl_4$, 골드 마이셀솔루션 얇은 하이브리드 필름을 만들기 위해서 스핀 코팅되었다. Annealing 이후에, 체인들이 재구성 되어지고, 체인이 구형 공중합체 필름을 형성한다. 나노파티클들이 강제로 형태학적 변화가 잇달아 일어나고 각각의 PEO 도메인으로 큰 single 전이되었다. $P3HT_{4k}$-b-$PFOMA_{14k}$, 의 경우는 마이크로 상분리와 자기블록 공중합체 마이크로상 분리와 자기조립, 그리고 블록공중합체는 마이셀 솔루션으로부터 추출한 모폴로지 같은 잘 구성된 나노섬유를 구성한다. 골드 나노파티클은 금 표면을 가진 P3HTs 의 황 원자

상호작용 때문에 안정화됩니다. 그리고 그들은 the P3HT phase 로 분산된다. 골드나노 파티클을 가진 마이셀 필름 안에서 thermal annealing, 솔벤트 annealing 과 초임계 이산화탄소 annealing 이후 나노 섬유의 길이가 증가되었습니다.

TABLE OF CONTENTS

LIST OF FIGURE

Chapter 1

GENERAL INTRODUCTION

1.1. BLOCK COPOLYMER

1.1.1. Molecular structure

Block copolymers, consisting of connected blocks (sequences) formed by two or more chemically homogenous polymer fragments joined together by covalent bonds, independent of the procedure of synthesis, can be in a linear and/or radial arrangement. In the simplest case, a diblock copolymer AB consists of two different homopolymers linked end to end. Extension of this concept leads to ABA or BAB triblocks and to $(AB)_n$ linear multiblocks, whereas ABC copolymers are obtained by the incorporation of a polymer sequence having a third composition. Radial arrangements of block copolymers are in the simplest case star-shaped structures, where *n* block copolymer chains are linked by one of their ends to a multifunctional moiety. Another structural possibility designated by heteroarm block copolymers is to link *n* homopolymer sequences to a given junction point [1]. The type of monomer in a block determines many of the properties and modern polymer synthetic techniques provide access to a wide range of components [2] (Figure 1.1). These block copolymers have shown great diversity in morphology, depending on the composition of block copolymer as well as the molecular architectures [3].

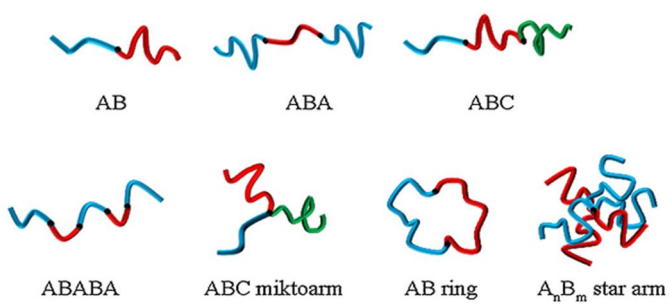

Figure 1.1. Various molecular architectures of block copolymers.

The complex structure of BCP materials leads to a variety of useful properties; indeed, industrial applications for BCPs in thermoplastic elastomers, foams, adhesives, etc. have been around for decades [4].

1.1.2. Diblock copolymer morphology

The phase behavior of diblock copolymers has been the subject of numerous theoretical and experimental studies over recent decades, and is relatively well understood [5-8]. This self-assembly process is driven by an unfavorable mixing enthalpy and a small mixing entropy, while the covalent bond connecting the blocks prevents macroscopic phase separation. The microphase separation of diblock copolymers depends on the total degree of polymerization N (= $N_A + N_B$), the Flory-Huggins χ-parameter (which is a measure of the incompatibility between the two blocks) and the volume fractions of the constituents blocks (f_A and f_B, $f_A = 1 - f_B$). The segregation product χN determines the degree of misrophase separation. Depending on χN, three different regimes can be distinguished: (1) the weak-segregation limit for $\chi N \leq 10$; (2) the intermediate segregation region for $10 < \chi N \leq 50$ and (3) the strong segregation limit for $\chi N \rightarrow \infty$.

Figure 1.2. Schematic representations of the morphologies obtained for diblock copolymer melts.

In bulk, the minority block is segregated from the majority block forming regularly-shaped and uniformly-spaced nanodomains [8]. The shape of the segregated domains in a diblock is governed by the volume fraction of the minority block, f, and block incompatibility. Figure 1.2 shows the equilibrium morphologies documented for diblock copolymers [9]. At the volume fraction of ≈ 20 %, the minority block forms a body-centred cubic spherical phase in the matrix of the majority block. It changes to hexagonally packed cylinders at a volume fraction ≈ 30 %. Alternating

lamellae are formed at approximately equal volume fractions for the two blocks. At the volume fraction of ≈ 38 %, the minority block forms gyroid or perforated layers at moderate and high incompatibility, respectively. Furthermore, the smallest dimension of a segregated domain, e.g., the diameter of a cylinder, is proportional to the two-thirds power of the molar mass of the minority block and can typically be tuned from ≈ 5 to ≈ 100 nm by changing the molar mass of the block [10].

1.1.3. Semifluorinated block copolymer

Semifluorinated block and graft copolymers are amphiphilic materials that combine the unique self-assembly characteristics of block copolymers and the unparalleled properties of fluorinated polymers. Fluorinated blocks have attracted much attention due to their unique such as low surface energy, excellent chemical and thermal stability, low refractive index and dielectric constant, chemical/biological inertness, and oil/water repellence, which cannot be achieved by the corresponding non-fluorinated materials [11-13]. They may be utilized in many applications for example, as surfactants for polyurethane foams [14] and as emulsifiers in liquid and supercritical carbon dioxide [15]. Although waterin-carbon dioxide (W/C) emulsions have been formed with perfluoroether surfactant and silicone based surfactants [16], they have not been reported with fluoromethacrylate polymers. These emulsions are of interest in environmentally benign solvent formulations for separations, polymerizations [17] and in material synthesis.

Lowering surface energy is mainly contributed by the structure and the hydrophobicity of the fluorinated copolymers. Perfluorinated segments of the fluorine containing graft copolymer of poly(perfluoroalkyl ethylmethacrylate)-graft-poly(methyl methacrylate) had better surface modification ability in comparison with the random copolymer with same components [18]. The reason is high hydrophobicity of graft copolymer and less hindrance of perfluoroalkyl groups by grafting methyl ester groups of methyl methacrylate segments.

Semifluorinated diblock copolymers based on methyl methacrylate and 1H, 1H, 2H, 2H-perfluoroalkyl methacrylates were prepared by

nucleophilic-catalyzed group transfer polymerization [19,20]. The surface activity of the materials and the formation of micelles were revealed in toluene. While the block copolymer formed cylindrical micelles, the coexistence of the poly(methyl methacrylate) homopolymer shifted the association equilibrium to the side of spherical aggregates. Micelles were formed with the fluorinated blocks turned inside the core and the non-fluorinated blocks located at the corona. However, the surface of thin polymer films cast from a toluene solution consisted mainly of the fluorinated block. During the film formation, monomeric polymers covered the surface with fluorinated block at the airside.

Several attempts have been reported to prepare semifluorinated copolymers by means of cationic [21], anionic [22], living radical [23], and group transfer polymerization [24], but few studies have addressed the synthesis of block copolymers composed of a hydrophilic block and a semifluorinated block [25,26]. The limited number of studies may be attributed to the limited solubility of fluorinated polymers in common organic solvents and the limited mechanisms by which the fluorocarbon monomer can be polymerized.

Controlled free radical polymerization techniques provide the best route for the preparation of these amphiphilic block copolymers due to the relative ease of synthesis and their compatibility with a wide range of solvents [27,28]. Specifically, atom transfer radical polymerisation (ATRP) is an attractive method for the synthesis of well-defined copolymers with controlled molecular weight, polydispersities, terminal functionalities, and chain architecture composition [28, 29].

Recently, the synthesis of block copolymers containing poly(ethylene oxide) (PEO) and PS were reported by ATRP using a PEO macro-initiator obtained by functionalizing the HO-PEO-OH with 2-bromo- or 2-chloropropionyl ester end group [30, 31]. The polymerization proceeded in a living manner to yield well-defined block copolymers, which are difficult to synthesize by the sequential anionic method. Thus, esterification of a hydroxyl group of a preformed macromolecule with halogenated acyl halide

proved to be an excellent method for producing macroinitiators suitable for ATRP [31, 32].

1.1.4 Conjugated rod-coil block copolymers

Several classes of π-conjugated rod-coil block copolymers have been reported in the literature, including fluorene [33-35], phenylene [36-38], thiophene [39-42], quinoline [43,44]. Aggregation and microphase separation of rod-coil block copolymers have yielded a number of nanoscale morphologies, such as lamellar, spherical, cylindrical, vesicular, and microporous structures. The π-π interaction between the conjugated rods provides additional structural control factor and functionality, which differs distinctly from those of conventional coil-coil block copolymers. Furthermore, the self-assembled morphology of conjugated rod-coil block copolymers may lead to additional electronic processes such as exciton confinement and interfacial effects. Also, the combination of a stimuli-responsive coil segment with the tunable photophysical properties of the conjugated rod could produce novel multifunctional sensory materials. The synthesis, morphology, and applications of conjugated rod-coil block copolymers involved in this review are summarized in Figure 1.3 [45].

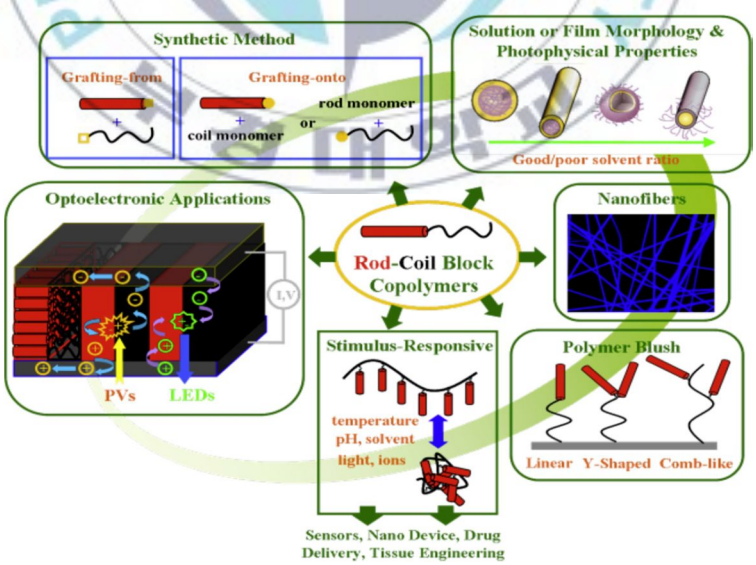

Figure 1.3. Synthesis, morphology, and applications of conjugated rod-coil block copolymers.

The self-assembly of rod-coil block copolymers is fundamentally different from that of coil-coil block copolymers because of the effect of chain topology on conformational entropy and molecular packing geometries and because of the additional interactions that can occur between anisotropic rod blocks. The rod block does not have the same conformational entropy as a coil block, which restricts its ability to stretch to accommodate packing within self-assembled structures and its ability to gain conformational entropy when dissolved in solution. The extended, anisotropic nature of the rodlike chains also leads to anisotropic interactions between the blocks, resulting in the potential for liquid crystalline ordering. In many rod-coil materials the rod blocks show not only liquid crystalline alignment but also extended chain crystalline phases or high-order smectics, further increasing the complexity of the systems [46-48].

1.1.5 Block copolymer containing regioregular poly(3-hexylthiophene)

Block copolymers consisting of stiff-rod and flexible-coil segments, referred to as 'rod-coil block copolymers', have been of great interest because of their specific properties, unexpected behavior and hierarchical nanostructures by self-assembly, as reported in several papers [49-51]. In particular, rod-coil block copolymers, based on π-conjugated rods such as poly(3-hexylthiophene) and poly(phenylene vinylene), have received much attention because of their prompt application to a wide variety of optoelectric devices.

McCullough *et al*. and Yokozawa *et al*. discovered that well-defined end-functionalized P3HTs can be synthesized with low polydispersity via a chain growth mechanism by using a catalyst-transfer polycondensation method mediated by a nickel catalyst (GRIM method) [52-54]. McCullough et al. further demonstrated that P3HT block copolymers can be synthesized from a linker molecule attached to an end-functionalized P3HT as a macroinitiator via atom transfer radical polymerization (ATRP) [55,56]. Recently, Tomoya Higashihara and coworkers reported new ABA-type coil-rod-coil triblock copolymers of PS-b-P3HT-b-PS [57] and PMMA-b-P3HT-b-PMMA [58]. In addition, attractive block copolymers comprised of donor-

acceptor segments have emerged, in which rod and coil segments correspond to P3HT and fullerene-substituted PS [59] or PMMA [60], respectively. New block copolymers bearing P3HT and poly(meth)acrylate substituted with perylene bisimide have also been developed [61,62].

1.2 ATOM TRANSFER RADICAL POLYMERIZATION

Atom transfer radical polymerization (ATRP) is an example of a living polymerization or a controlled/living radical polymerization. ATRP is an attractive method for the synthesis of well-defined copolymers with controlled molecular weight, polydispersities, terminal functionalities, and chain architecture composition. ATRP is a tool for the formation of carbon-carbon bonds in organic synthesis. As the name implies, the atom transfer step is the key step in the reaction responsible for uniform polymer chain growth. ATRP (or transition metal-mediated living radical polymerization) was independently discovered by Mitsuo Sawamoto [63] and by Krzysztof Matyjaszewski and Jin-Shan Wang in 1995 [64]. A general mechanism for ATRP shown in Scheme 1.1.

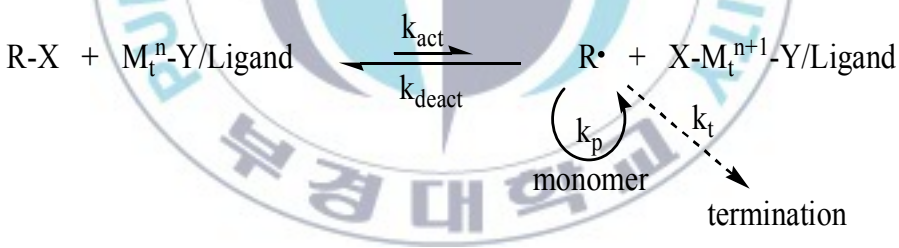

Scheme 1.1. Transition-Metal-Catalyzed ATRP

The radicals, or the active species, are generated through a reversible redox process catalyzed by a transition metal complex (M_t^n-Y/Ligand, where Y may be another ligand or the counterion) which undergoes a one-electron oxidation with concomitant abstraction of a (pseudo)halogen atom, X, from a dormant species, R-X. This process occurs with a rate constant of activation, k_{act}, and deactivation k_{deact}. Polymer chains grow by the addition of the intermediate radicals to monomers in a manner similar to a conventional radical polymerization, with the rate constant of propagation k_p.

Termination reactions (k_t) also occur in ATRP, mainly through radical coupling and disproportionation; however, in a well-controlled ATRP, no more than a few percent of the polymer chains undergo termination. Other side reactions may additionally limit the achievable molecular weights. Typically, no more than 5% of the total growing polymer chains terminate during the initial, short, nonstationary stage of the polymerization. This process generates oxidized metal complexes, $X\text{-}M_t^{n+1}$, as persistent radicals to reduce the stationary concentration of growing radicals and thereby minimize the contribution of termination [65]. A successful ATRP will have not only a small contribution of terminated chains, but also a uniform growth of all the chains, which is accomplished through fast initiation and rapid reversible deactivation.

The name atom transfer radical polymerization originates from the atom transfer step, which is the key elementary reaction responsible for the uniform growth of the polymeric chains, in the same way that the addition-fragmentation is the key step in the RAFT process. ATRP has its roots in atom transfer radical addition (ATRA), which targets the formation of 1:1 adducts of alkyl halides and alkenes, also catalyzed by transition metal complexes [66]. ATRA is a modification of Kharasch addition reaction, which usually occurs in the presence of light or conventional radical initiators [67]. Because of the involvement of transition metals in the activation and deactivation steps, chemo-, regio-, and stereoselectivities in ATRA and the Kharasch addition may be different. For example, under Kharasch conditions, in the reaction with chloroform the alkene will "insert" across the $H\text{-}CCl_3$ bond but in ATRA it will insert across the $Cl\text{-}CHCl_2$ bond, because the C-Cl bond is rapidly activated by the Fe(II) or Cu(I) complexes [68].

ATRP also has roots in the transition metal catalyzed telomerization reactions [69]. These reactions, however, do not proceed with efficient exchange, which results in a nonlinear evolution of the molecular weights with conversions and polymers with high polydispersities. ATRP also has connections to the transition metal initiated redox processes as well as inhibition with transition metal compounds [70-72]. These two techniques

allow for either an activation or deactivation process, however, without efficient reversibility. ATRP was developed by designing an appropriate catalyst (transition metal compound and ligands), using an initiator with the suitable structure, and adjusting the polymerization conditions such that the molecular weights increased linearly with conversion and the polydispersities were typical of a living process [73-75]. This allowed for an unprecedented control over the chain topology (stars, combs, branched), the composition (block, gradient, alternating, statistical), and the end functionality for a large range of radically polymerizable monomers [76-80]. Earlier attempts with heterogeneous catalyst and inefficient initiators were less successful [81].

ATRP reactions are very robust in that they are tolerant of many functional groups like allyl, amino, epoxy, hydroxy and vinyl groups present in either the monomer or the initiator [82]. ATRP methods are also advantageous due to the ease of preparation, commercially available and inexpensive catalysts (copper complexes), pyridine based ligands and initiators (alkyl halides) [83]. A very attractive feature of ATRP is that it combines the advantages of controlled molecular weight and low polydispersity offered by anionic living polymerization with the ease of a free-radical polymerization. The requirement of achieving extremely pure polymerization conditions that limits the general applicability of anionic living polymerization is not an issue in ATRP.

1.3. NANOPARTICLES AND POLYMERIC NANOCOMPOSITES

1.3.1. Nanoparticles

Nanoparticles are defined as particles with size in the range of 1 to 100 nm at least in one of the three dimensions. In this size range, the physical, chemical and biological properties of the nanoparticle change in fundamental ways from the properties of both individual atoms/molecules and of the corresponding bulk material. Nanoparticles can be made of materials of diverse chemical nature, the most common being metals, metal oxides, silicates, non-oxide ceramics, polymers, organics, carbon and biomolecules. Nanoparticles exist in several different morphologies such as

spheres, cylinders, platelets, tubes, etc. Generally, they are designed with surface modifications tailored to meet the needs of specific applications they are going to be used for. The enormous diversity of the nanoparticles (Figure 1.4) arising from their wide chemical nature, shapes and morphologies, the medium in which the particles are present, the state of dispersion of the particles and most importantly, the numerous possible surface modifications the nanoparticles can be subjected to make this an important active field of science [84].

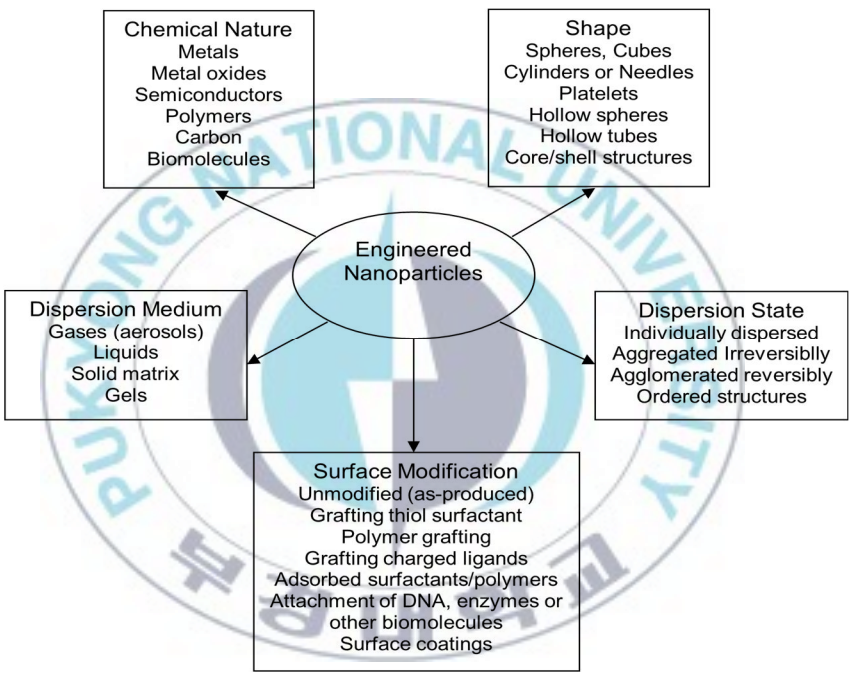

Figure 1.4. Various features contributing to the diversity of engineered nanoparticles. The same chemical can generate a wide variety of nanoparticles.

The most significant consequences of the nanoscale are the presence of a high fraction of atoms/molecules constituting the nanoparticle on the particle surface rather than in the particle interior and the immense surface area available per unit volume of the material. Both of these properties increase in magnitude with a decreasing particle size. The unique physical, chemical and biological properties of nanomaterials originate from these

two features. In some nanoscale materials quantum effects are exhibited allowing for a number of interesting applications. Further, unusual morphologies such as carbon nanotubes (CNT) and dendrimers contribute to morphology dependent novel applications [84].

The small particle size leads to many unique properties of nanoparticles. Nanoparticles display interesting optical properties since the absorption and/or emission wavelengths can be controlled by particle size and surface functionalization. If the nanoparticle size is below the critical wavelength of light, then transparency can be attained. The chemical nature and the size of the nanoparticle control the ionic potential or the electron affinity and thereby the electron transport properties. For metals, with decreasing size of nanoparticles, the sintering and melting temperatures decrease. Nanoparticles may be incorporated into a solid matrix to provide better thermal conduction. For some metals and metal oxides, the decrease of the particle size results in improved magnetic behavior. Individual metallic magnetic nanoparticles can exhibit super paramagnetic behavior [84].

The large specific surface area of nanoparticles is the origin of a number of their unique applications. Catalysis is enhanced by high surface area per unit volume and the homogenous distribution of nanoparticles. High surface areas give strong interactions between the nanoparticles and the solid matrix in which they may be incorporated. In composites, depending on the chemistry of the nanoparticle, its aspect ratio, extent of dispersion and interfacial interactions with the polymer matrix (which can be modified by surface functionalization), it is possible to obtain different levels of mechanical properties for the final composites. In particular, a high elastic modulus can be achieved without a proportional loss in impact strength that is commonly observed when larger particles are used. The platelet morphology and large specific surface areas of silicate particles enhance the barrier properties of polymer membranes by vastly increasing the pathway for molecular transport of permeating substances. Nanoparticles can also influence the flammability of polymers by increasing the glass transition temperature and the heat deflection temperature.

For most practical applications, the nanoparticles have to be assembled in one, two or three dimensions, similar to how atoms and molecules are assembled into matter. For example, a sensing device may require that nanoparticles be arranged with specified inter-particle separation. An optoelectronic device may require the nanoparticles to be assembled to create a patterned surface. In general, it will be necessary to place the nanoparticles in specified locations on a substrate so that addressing and connecting them to the macroscopic outside world will be possible.

Figure 1.5. Assembling nanoparticles for applications, (a) Nanoparticles with stabilizing polymer molecules around them in a random three dimensional arrangement to create a porous nanoparticle system for catalytic or adsorption applications, (b) Nanoparticles assembled on a polyelectrolyte or a DNA molecule to serve as a nanoelectrical wire, (c) Nanoparticles assembled on a block copolymer patterned surface with nanoparticles located at the domain boundaries for a sensor application [85].

A number of approaches have been developed to accomplish this objective. For example, surface patterning has been used to direct polymer and silica nanoparticles to specific surface locations. Self-assembled surfactant and block copolymer nanostructures have been used as templates to direct the nanoparticle assembly of metal oxide particles to generate mesoporous materials. Cationic (or anionic) polyelectrolytes have been used to direct the assembly of oppositely charged nanoparticles such as negatively charged gold particles or silica particles. Nanoparticles can also self-assemble into nano-crystalline materials. A variety of molecular recognition methods such as antigen-antibody interactions have been used to

direct the assembly of nanoparticles that have the recognition molecules bound to their surfaces. The binding of DNA to the nanoparticle surface has been used to create particle assemblies dictated by nucleic acid interactions. Nanoparticles have also been self-assembled at air-liquid and liquid-liquid interfaces taking advantage of surface tension effects. Also the dewetting of a solid surface by a polymer solution has been exploited to attain nanoparticle self-assembly. Biological nanoparticles such as viruses can self-assemble to yield ordered nanoparticle assemblies in one, two or three dimensions.

Nanoparticles constitute the building blocks for nanotechnology and thus for numerous potential applications in energy and power, health and biomedicine, electronics and computers, environmental applications, new engineering materials, consumer goods, personal care products, food and transportation. To perform these functions nanoparticles have to be synthesized, passivated to control their chemical reactivity, stabilized against particle aggregation, and functionalized to achieve specific performance goals. The individual nanoparticles then have to be assembled into devices or integrated into other solid matrices to create the final nanoproducts. The tremendous diversity of nanoparticles possible because of their wide chemical nature, shape and morphology, medium in which they are present, their state of dispersion and the nature of surface modifications make this a rich field for scientific investigations.

1.3.2. Gold nanoparticles

Gold nanoparticles (AuNPs) have long been a topic of intense research due to their size-related electromagnetic, optical and catalysis properties [86,87]. These properties are significantly different from those of the corresponding bulk materials or molecular compounds, resulting in a wide range of applications in such fields as optoelectronics, biology and catalysis [86-88]. Bare gold nanoparticles are not stable and prone to aggregate into bulk materials, thus stabilizing agents have been used to decorate their surface. Polymers as stabilizers for gold nanoparticles have attracted increasing interest since they exhibit many advantages, such as enhancing the long-term stability of gold nanoparticles, tuning the solubility and

amphiphilicity of gold nanoparticles, promoting the compatibility and processability of gold nanoparticles, giving gold nanoparticles special properties, etc [89].

In typical synthesis, AuNPs are produced by reduction of gold salts such as $AuCl_3$ in an appropriate solvent. Usually a stabilizing agent is also added to prevent the particles from aggregating. Because thiol groups bind to gold surfaces with high affinity, most frequently thiol-modified ligands are used as stabilizing agents which bind to the surface of the AuNPs by formation of Au-sulfur bonds [90]. Synthesis of AuNPs with various sizes and shapes can be achieved through judicious choice of experimental conditions and additives [91-93]. Several mechanisms have been proposed to explain the dependence of the morphology and geometry of AuNPs on the growth conditions. However, none of these mechanisms is widely accepted [94].

After synthesis, the stabilizing agents surrounding the AuNPs can be replaced by other molecules by ligand exchange reactions [95]. In addition, ligands can also be linked to the shell of stabilizing agents. One of the most common applications is the linkage of amino groups in biological molecules with carboxyl groups at the free ends of the stabilizing agents [96]. Functionalization of AuNPs makes it possible to adjust the surface properties and attach different kinds of molecules to the particles.

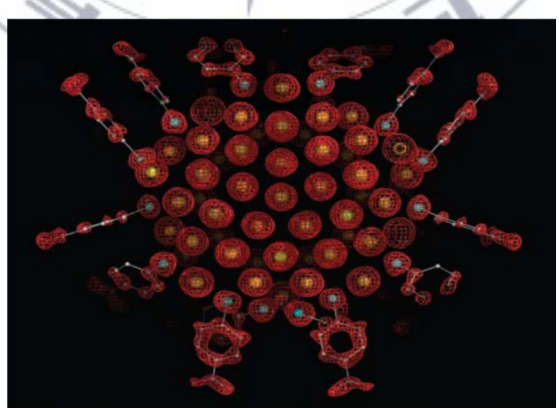

Figure 1.6. Electron density map (red mesh) and atomic structure (gold atoms depicted as yellow spheres, and p-MBA shown as framework and with small spheres) of $Au_{102}(p\text{-}MBA)_{44}$.

Jadzinsky *et al*. reported a crystal structure of a thiol monolayer-protected AuNP, which contains 102 gold atoms and 44 p-mercaptobenzoic acid (p-MBA) units [97]. This is the first detailed structural study of nanometer-sized AuNPs. The nanoparticles are chiral, although they crystallize in the centrosymmetric space group C2/c. The gold atoms in the core are packed in a Marks decahedron, whereas the thiol monolayer outside is stabilized by both gold-sulfur bonding and interactions between p-MBA molecules.

AuNPs have shown great potential applications in the fields of chemistry, physics, materials, biology, medicine, and related interdisciplinary fields [98-100]. Zhou *et al*. reported a method to detect copper(II) by azide- and alkyne-functionalized AuNPs based on the fact that the extinction efficient of gold nanoparticles is several orders of magnitude larger than those of traditional organic chromophores [101]. The 50 μM minimum concentration sets the record for detection of Cu^{2+} by the naked eye. Another exciting finding is that AuNPs have shown potential in therapies for HIV [102]. By attaching multiple copies of a low acting HIV drug onto AuNPs, Bowman and his coworkers have stopped HIV from infecting human white blood cells. The results demonstrate that we may find a simple strategy to convert therapeutically poorly active monovalent small organic molecules into highly active drugs by just conjugating them to AuNPs.

1.3.3. Nanoparticle-Polymer Composites

Nanoparticle-polymer composites are commonly defined as a binary mixture of functional inorganic nanomaterials dispersed in a polymeric matrix. Inorganic materials with a characteristic size on the nanometer scale can give various functionalities with unique electric, magnetic, and optical properties while the polymer matrix allows the integration and stability of nanomaterials as well as processability. Moreover, nanocomposites of polymer and inorganic nanoparticles can exhibit new properties that are not possessed by the components in their own right. A large number of research works have been presented in the literature that were dedicated to technological and scientific problems of polymeric nanocomposites, and, as a result, the combination of such kinds of materials enables nanocomposites

to be used in wide fields ranging from microelectronics to biomedical applications [103-107].

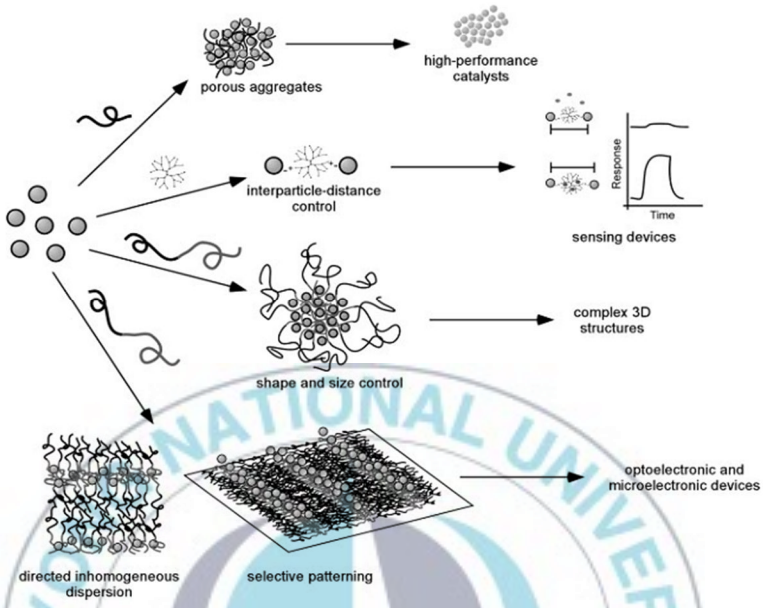

Figure 1.7. Polymer-mediated assembly approaches to fabrication of ordered nanocomposites and their possible utilization.

Several experimental methods have been developed for incorporating inorganic nanoparticles into polymeric nanostructures [108-119]. The most popular approach involves the synthesis of nanoparticles in situ within the block copolymer template by using preformed micelles of block copolymers containing metal precursors. However, despite the importance of controlling the arrangement of nanoparticles produced by such methods within the periodic structure of the block copolymer, establishing such control has been difficult. Another approach, recently proposed as a possible way to overcome some of these drawbacks, uses cooperative selforganization of preformed nanoparticles and block copolymers. After the preparation of the nanoparticles, the particle core size was the significant parameter in the localization of particles along the interface between the two blocks or at the center of the respective polymer domain. The localization is limited by two

factors: the size of the particles deposited on the surface and the width of the interface between neighboring polymer blocks [120].

Polymer-mediated nanoparticle assembly provides a versatile and effective method for the creation of structured nanocomposite materials where control over composite morphology is paramount. In addition to their role in assembling nanoparticles, functionalized polymers can be used to control interparticle distances, assembly shape, size and porosity, and to induce an anisotropic ordering of nanoparticles. The ability to control such structural parameters enables the creation of responsive materials as well as effective catalysts.

1.4 AIM AND OUTLINE OF THIS THESIS

The main thrust of this thesis is to investigate a simple *in situ* synthesis of gold nanoparticles in semifluorinated block copolymer thin films. The organization of inorganic nanostructures within self-assembled organic or biological templates is receiving the attention of scientists interested in developing functional hybrid materials. So, the studies carried out in this thesis are basically divided into two parts. In the first part, the preparation of gold nanoparticles incorporated in self-assembled and ordered poly(1H,1H-dihydroperfluorooctyl methacrylate)-*b*-polyethylene oxide (PFOMA-*b*-PEO) block copolymer thin films is explored. Herein, the approaches for preparing the well-ordered Au/polymer hybrid structures are discussed, which employ thermal annealing, solvent annealing and supercritical CO_2 process.

In the second part of the thesis, thin nanocomposite films generated from poly(3-hexylthiophene)-b-poly(fluorooctyl methacrylate) (P3HT-b-PFOMA) micellar solution in which gold precursor was added, were also investigated. The microphase separation and self-assembly behavior of the block copolymer was studied. The development of the morphology of Au-loaded micellar solution of P3HT-*b*-PFOMA was investigated after annealing in solvent vapor and also in supercritical CO_2.

1.5 REFERENCES

1. R. Gérard, *Prog.Polym.Sci.28*, 1107-1170, 2003.
2. I. W. Hamley, "The Physics of Block Copolymers," *Oxford University Press*, New York, 1998.
3. J. K. Kim, S. Y. Yang, Y. Lee and Y. Kim, *Progress in Polymer Science 35*, 1325-1349, 2010.
4. S.B. Darling, *Prog. Polym. Sci. 32*, 1152-1204, 2007.
5. L. Leibler, *Macromolecules 13*, 1602, 1980.
6. F. S. Bates, *Science 251*, 898, 1991.
7. G. H. Fredrickson, F. S. Bates and Annu, *Rev. Mater. Sci. 26*, 501, 1996.
8. H. A. Klok and S. Lecommandoux, *Adv. Mater. 13*, 1217, 2001.
9. A. K. Khandpur, S. Foerster, F. S. Bates, I. W. Hamley, A. J. Ryan, W. Bras, K. Almdal and K. Mortensen, *Macromolecules 28*, 8796, 1995.
10. F. S. Bates and G. H. Fredrickson, *Phys. Today 52*, 32, 1999.
11. Z. B. Zhang, S. K. Yinga and Z. Q. Shi, *Polymer* 40, 5439, 1999.
12. T. Imae, *Current Opinion in Colloid and Interface Science* 8, 307, 2003.
13. A. Hirao, K. Sugiyama and H. Yokoyama, *Prog. Polym. Sci. 32,* 1393, 2007.
14. M. J. Krupers, C. F. Bartelink, H. J. M. Grunhauer and M. Moller, *Polymer* 39(10), 2049-53, 1998.
15. J. L. Kendall, D. A. Canelas, J. L. Young and J. M. De. Simone, *Chem Rev 99,* 2, 543-563, 1999.
16. R. D. Butler, M. Cait and A. I. Cooper, *Adv Mater. 13*, 1459-1463, 2001.
17. V. Percec and M. Lee, *J. Macromol Sci, Pure Appl Chem A29,* 9, 723-740, 1992.
18. I. J Park, S. B. Lee and C. K. Choi, *Macromolecule 31*, 7555 -7558, 1998.
19. M. J. Krupers and M. Moller, *Macromol Chem Phys 198*, 2163 - 2179, 1997.
20. M. J. Krupers, S. S. Sheiko and M. Moller, *Poly Bul 40*, 211- 217, 1998.

21. V. Percec and M. Lee, *J. Macromol Sci, Pure Appl. Chem. A29,* 9, 723-740, 1992.

22. D.R. Iyengar, S.M. Perutz, C.A. Dai, C.K. Ober and E.J. Kramer *Macromolecules 29*, 1229-1234, 1996.

23. D. E. Betts, T. Johnson, D. LeRoux and J. M. DeSimone, *ACS Symposium Series ACS Symposium Series 685*, 418-432, 1998.

24. M. J. Krupers, S. S. Sheiko and M. Möller, *Polym Bull 40*, 211-217, 1998.

25. M. Miyamoto, K. Aoi and T. Saegusa, *Macromolecules 22*, 3540-3543, 1989.

26. K. Matsumoto, H. Mazaki, R. Nishimura, H. Matsuoka and H. Yamaoka, *Macromolecules 33*, 8295-8300, 2000.

27. Z. Guan and J. M. De. Simone, *Macromolecules 27*, 5527-5532, 1994.

28. T. E. Patten and K. Matyjaszewski, *Adv Mater 10*, 12, 901-915, 1998.

29. J. Ueda, M. Matsuyama, M. Kamigaito and M. Sawamoto, *Macromolecules 31* 3, 557-562, 1998.

30. K. Jankova, X. Chen, J. Kops and W. Batsberg, *Macromolecules 31*, 538-541, 1998.

31. K. Jankova, J.H. Truelsen, X. Chen, J. Kops and W. Batsberg, *Polym Bull 42*, 153-158, 1999.

32. H. Kim, L. Bes, D.M. Haddleton and E. Khoshdel, *J Polym Sci, Part A: Polym Chem 39*, 1833-1842, 2001.

33. D. Marsitzky, M. Klapper and K. Mullen, *Macromolecules* 32, 8685-8, 1999.

34. M. Surin, D. Marsitzky, A. C. Grimsdale, K. Mullen, R. Lazzaroni and P. Leclere, *Adv Funct Mater 14*, 708-15, 2004.

35. Y. C. Tung, W. C. Wu and W. C. Chen, *Macromol Rapid Commun 27*, 1838-1844, 2006.

36. C. Brochon, N. Sary, R. Mezzenga, C. Ngov, F. Richard, M. May and G. Hadziioannou, *J. Appl. Polym. Sci. 110*, 3664-3670, 2008.

37. U. Stalmach, B. de. Boer, A. D. Post, P. F. van Hutten and G. Hadziioan- nou, *Angew Chem Int Ed 40*, 428-430, 2001.

38. B. De Boer, U. Stalmach, H. Nijland and G. Hadziioannou, *Adv Mater 12*, 1581-1583, 2000.

39. F. Richard, C. Brochon, N. Leclerc, D. Eckhardt, T. Heiser and G. Hadziioan- nou, *Macromol Rapid Comm 29*, 885-891, 2008.

40. C. A. Dai, W. C. Yen, Y. H. Lee, C. C. Ho and W. F. Su, *J Am Chem Soc 129*, 11036-11038, 2007.

41. J. Zou, L. Liu, H. Chen, S. I. Khondaker and R. D. McCullough RD, Huo Q, Zhai L. *Adv Mater 20*, 2055-2060, 2008.

42. J. Liu, E. Sheina, T. Kowalewski and R. D. McCullough, *Angew Chem Int Ed 41*, 329-332, 2002.

43. S. A. Jenekhe and X. L. Chen, *Science 279*, 1903-1907, 1998.

44. S. A. Jenekhe and X. L. Chen, *Science 283*, 372-375, 1999.

45. C. L. Liu, C. H. Lin, C. C. Kuo, S. T. Lin and W. C. Chen, *Polymer,* 2010.

46. V. Pryamitsyn and V. Ganesan, *Journal of Chemical Physics* 120, 5824-5838, 2004.

47. A. N. Semenov, S. V. Vasilenko, Z. Eksperimentalnoi and I. T. Fiziki, 90, 124-140, 1986.

48. M. W. Matsen and C. Barrett, *Journal of Chemical Physics 109*, 4108-4118, 1998.

49. S. A. Jenekhe and X. L. Chen, *Science 283*, 372-375, 1999.

50. H. A. Klok and S. Lecommandoux, *Adv. Mater. 13*, 1217-1229, 2001.

51. Lee, M., Cho, B.- K. & Zin, W.-C. *Chem. Rev. 101*, 3869-3892, 2001.

52. M. C. Iovu, E. E. Sheina, R. R. Gil and R. D. McCullough, *Macromolecules 38*, 8649, 2005.

53. M. Jeffries-EL, G. Sauve and R. D. McCullough, *Macromolecules 38*, 10346, 2005.

54. R. Miyakoshi, A. Yokoyama and T. Yokozawa, *J. Am. Chem. Soc. 127*, 17542, 2005.

55. J. S. Liu, E. Sheina, T. Kowalewski and R. D. McCullough, *Angew. Chem., Int. Ed. 41*, 329, 2002.

56. M. C. Iovu, M. Jeffries-El, E. E. Sheina, J. R. Cooper and R. D. McCullough, *Polymer 46*, 8582, 2005.

57. T. Higashihara, K. Ohshimizu, A. Hirao and M. Ueda, *Macromolecules 41*, 9505-9507, 2008.

58. T. Higashihara and M. Ueda, *React. Funct. Polym. 69*, 457-462, 2009.

59. F. Richard, C. Brochon, N. Leclerc, D. Eckhardt, T. Heiser and G. Hadziioannou, *Macromol. Rapid Commun. 29*, 885-891, 2008.

60. J. U. Lee, A. Cirpan, T. Emrick, T. P. Russell and W. H. Jo, *J. Mater. Chem. 19*, 1483-1489, 2009.

61. M. Sommer, A. S. Lang and M. Thelakkat, *Angew. Chem., Int. Ed. 47*, 7901-7904, 2008.

62. Q. Zhang, A. Cirpan, T. P. Russell and T. Emrick, *Macromolecules 42*, 1079-1082, 2009.

63. M. Kato, M. Kamigaito, M. Sawamoto and T. Higashimura, *Macromolecules* 28, 1721, 1995.

64. J. Wang and K. Matyjaszewski, *J. Am. Chem. Soc.* 117, 5614, 1995.

65. H. Fischer, *J. Polym. Sci., Part A: Polym. Chem. 37*, 1885, 1999.

66. D. P. Curran, *Synthesis,* 489, 1988.

67. M. S. Kharasch and E. V. Jensen, *Science 102*, 128, 1945.

68. F. Minisci, *Acc. Chem. Res. 8*, 165, 1975.

69. B. Boutevin, *J. Polym. Sci., Part A: Polym. Chem. 38*, 3235, 2000.

70. C. H. Bamford, *Comprehensive Polymer Science*, G. Allen, S. L. Aggarwal, S. Russo, Eds.; Pergamon: Oxford, Vol. 3,123, 1989.

71. K. Matyjaszewski and J. Xia, *Chemical Reviews 101*, No. 9, 2985, 2001.

72. J. Qiu and K. Matyjaszewski, *Acta Polym. 48*, 169, 1997.

73. K. Matyjaszewski and J. S. Wang, WO Pat. 9630421, U.S. Pat. 5, 763, 548.

74. J. S. Wang and K. Matyjaszewski, *Macromolecules 28*, 7901, 1995.

75. V. Percec and B. Barboiu, *Macromolecules 28*, 7970, 1995.

76. K. Matyjaszewski, S. Coca, S. G. Gaynor, D. Greszta, T. E. Patten, J. S. Wang and J. Xia, WO Pat. 9718247, U.S. Pat. 5,807, 937.

77. K. Matyjaszewski, S. Coca, S. G. Gaynor, Y. S. Nakagawa and M. Jo, WO Pat. 9801480, U.S. Pat. 5, 789, 487.

78. T. E. Patten and K. Matyjaszewski, *Adv. Mater. 10*, 901, 1998.

79. K. Matyjaszewski, *Chem. Eur. J. 5*, 3095, 1999.

80. T. E. Patten and K. Matyjaszewski *Acc. Chem. Res. 32*, 895, 1999.

81. T. Otsu, Tazaki and M. Yoshioka, *Chem. Express 5*, 801, 1990.

82. J. M. G. Cowie and V. Arrighi, *CRC Press Taylor and Francis Group*: Boca Raton, Fl, 3rd Edition, 82-84, 2008.

83. K. Matyjaszewski, *Fundamentals of ATRP Research*, 2009.

84. R. Nagarajan, *ACS Symposium Series, American Chemical Society*: Washington, DC, 2008.

85. R. Shenhar, T. B. Norsten and V. M. Rotello, *Adv. Mater. 17 (6)*, 657, 2005.

86. M. C. Daniel and D. Astruc, *Chem. Rev. 104*, 293, 2004.

87. G. J. Hutchings, M. Brust and H. Schmidbaur, *Chem. Soc. Rev. 37*, 1759, 2008.

88. A. S. K. Hashmi, *Chem. Rev. 107*, 3180, 2007.

89. J. Shan and H. Tenhu, *Chem. Commun.* 4580, 2007.

90. A. C. Templeton, W. P. Wuelfing, R. W. Murray, *Acc. Chem. Res. 33*, 27-36, 2000.

91. H. Liao, Y. Jiang, Z. Zhou, S. Chen and S. Sun, *Angew. Chem. Int. Ed. 47*, 9100-9103, 2008.

92. S. S. Shankar, A. Rai, B. Ankamwar, A. Singh, A. Ahmad, M. Sastry, *Nature Materials 3*, 482-488, 2004.

93. K. L. McGilvray, M. R. Decan, D. Wang and J. C. Scaiano, *J. Am. Chem. Soc. 128*, 15980-15981, 2006.

94. C. Lofton and W. Sigmund, *Adv. Funct. Mater. 15*, 1197-1208, 2005.

95. T. Pellegrino, S. Kudera, T. Liedl, A. M. Javier, L. Manna and W. J. Parak, *Small 1*, 48-63, 2005.

96. R. A. Sperling, T. Pellegrino, J. K. Li, W. H. Chang and W. J. Parak, *Adv. Funct. Mater. 16*, 943-948, 2006.

97. P. D. Jadzinsky, G. Calero, C. J. Ackerson, D. A. Bushnell and R. D. Kornberg, *Science* 318, 430-433, 2007.

98. J. Yang, K. Eom, E. Lim, J. Park, Y. Kang, D. S. Yoon, S. Na, E. K. Koh, J. Suh, Y. Huh, T. Y. Kwon and S. Haam, *Langmuir 24*, 12112-12115, 2008.

99. J. D. Gibson, B. P. Khanal and E. R. Zubarev, *J. Am. Chem. Soc. 129*, 11653-11661, 2007.

100. Y. C. Cao, R. Jin and C. A. Mirkin, *Science 297*, 1536-1540, 2007.

101. Y. Zhou, S. Wang, K. Zhang and X. Jiang, *Angew. Chem. Int. Ed. 47*, 7454-7456, 2008.

102. M. Bowman, T. E. Ballard, C. J. Ackerson, D. L. Feldheim, D. M. Margolis and C. J. Melander, *Am. Chem. Soc. 130*, 6896-6897, 2008.

103. Y. W. Mai and Z. Z. Yu, *Cambridge: Woodhead Publishing* Ltd., 2006.

104. D. R. Paul and L. M. Robeson, *Polymer 49(15)*, 3187-204, 2008.

105. G. V. Ramesh, S. Porel, T. P. Radhakrishnan, *Chem Soc Rev 38(9)*, 2646-2656, 2009.

106. Y. Y. Wu, G. S. Cheng, K. Katsov, S. W. Sides, J. F. Wang and J. Tang, *Nat Mater. 3 (11)*, 816-822, 2004.

107. G. Reiss and A. Hütten , *Nat. Mater. 4(10)*, 725-726, 2005.

108. M. R. Bockstaller, Y. Lapetnikov, S. Margel, E. L. Thomas, *J. Am. Chem. Soc. 125*, 5276-5277, 2003.

109. M. R. Bockstaller, R. A. Mickiewicz and E. L. Thomas, *Ad*V. *Mater. 17*, 1331-1349, 2005.

110. J. J. Chiu, B. J. Kim, E. J. Kramer and D. J. Pine, *J. Am. Chem. Soc. 127*, 5036-5037, 2005.

111. Y. Boontongkong and R. E. Cohen, *Macromolecules 35*, 3647- 3652, 2002.

112. B. J. Kim, J. J. Chiu, G. R. Yi, D. J. Pine and E. J. Kramer, *Ad*V. *Mater. 17*, 2618-2622, 2005.

113. R. S. Kane, R. E. Cohen, R. Silbey, *Chem. Mater. 11*, 90-93, 1999.

114. Y. Lin, A. Boker, J. B. He, K. Sill, H. Q. Xiang, C. Abetz, X. F. Li, J. Wang, T. Emrick, S. Long, Q. Wang, A. Balazs and T. P. Russell, *Nature (London) 434*, 55-59, 2005.

115. M. J. Misner, H. Skaff, T. Emrick and T. P. Russell, *Ad*V. *Mater. 15*, 221-224, 2003.

116.V. Sankaran, J. Yue, R. E. Cohen, R. R. Schrock, R. J. Silbey, *Chem. Mater. 5*, 1133-1142, 1999.

117.J. Spatz, S. Mossmer, M. Moller, M. Kocher, D. Neher and G. Wegner, *Ad*V. *Mater. 10*, 473-475, 1998.

118.W. A. Lopes and H. M. Jaeger, *Nature (London) 414*, 735-738, 2001.

119.K. Tsutsumi, Y. Funaki, Y. Hirokawa and T. Hashimoto, *Langmuir 15*, 5200-5203, 1999.

120.A. Haryono and W. H. Binder, *Small 2*, No. 5, 600-611, 2006.

Chapter 2

SINTERING OF NANOPARTICLES THROUGH PHASE TRANSITION OF BLOCK COPOLYMERIC MICELLAR THIN FILMS

The preparation of gold nanoparticles incorporated in self-assembled and ordered poly(1H,1H-dihydroperfluorooctyl methacrylate)-*b*-polyethylene oxide (poly(FOMA-*b*-EO)) block copolymer thin films is explored with a change of size of the gold nanoparticles through a phase transition. Semifluorinated diblock copolymers poly($FOMA_{10k}$-*b*-EO_{12k}) was prepared by atom transfer radical polymerization (ATRP), and its micellar solution with a gold precursor, $LiAuCl_4$, in chloroform was spin-coated onto substrate to produce thin hybrid films. The salts complexed with the PEO chains selectively. Three different annealing modes of $LiAuCl_4$-loaded block copolymeric thin films were employed: in solvent vapor annealing at 70 ^{0}C, in supercritical CO_2 at 70 ^{0}C and in a vacuum oven at 100 ^{0}C. After annealing, the chains was reorganized as they try to reach thermodynamic equilibrium and formed spherical copolymeric films. The nanoparticles were forced to follow the morphological change and were transformed into a larger single particle in each PEO domain.

2.1. INTRODUCTION

Over the last few decades, many approaches have been made to synthesize metallic or semiconductor nanoparticles using block copolymers as templates or nanoreactors in order to modify the unique optical, magnetic, electronic, and catalytic properties [1,2]. In particular, gold nanoparticles have attracted much interest for applications as catalysts, chemical sensing and as well as building blocks for electronic devices that operate at the single-electron level [3-5]. The fabrication of thin layers is essential for such applications and control over the location at the nanoscale will be the key for the manipulation of the certain properties of the nanocomposite systems. Selective loading is an essential condition, in which the number of nanoparticles is controlled in the desirable blocks, because physical and chemical properties are mainly determined by how metallic nanoparticles are dispersed in the designed polymer structures.

The incorporation of nanoparticles into block copolymer domains can be done in two ways. In the first, the nanoparticles having uniform size and shape are synthesized separately and then mixed with the block copolymer to generate polymeric nanocomposites (e*x situ* method) [6-8]. For example, Kramer and coworkers examined to incorporate nanoparticles and control their location within different diblock copolymer domains by controlling the surface chemistry of the particles [6]. Wei and coworkers examined the morphological transformation from cylinder phase to lamellar phase in poly((styrene)-block-4-vinylpyridine) (PS-b-P4VP) diblock copolymers through the hybridization with modified CdS quantum dots [7]. Green and coworkers recently reported that polystyrene functionalized gold nanocrystals were initially dispersed within the corona PS phase of the polystyrene-*b*-poly(1,1,2,2-tetrahydroperflurooctyl methacrylate) (PS-*b*-PFOMA) block copolymer. Upon annealing in $scCO_2$, the structure inverted and the PS chains subsequently constituted the core, harboring the nanocrystals closer to the block interface, with the PFOMA chains forming a continue (corona) phase [8]. In this case, it is easy to control the shape and size of nanoparticles through separate synthesis, but difficult to make well-ordered dispersion in the polymer matrix due to the lack of interaction

between nanoparticles and polymers. In the other way, the inorganic precursors are mixed with block copolymer in solution, and then self-assembled together to form the nanocomposites with better dispersion of inorganic nanoparticles through reduction process (*in situ* method) [9-14]. For example, Sohn and coworkers demonstrated core-corona inversion of micelles was induced *in situ* in a free-standing film by a selective solvent for the core and applied this inversion of micelles to silver nanoparticles [9]. Ho and coworkers investigated morphological evolution by the introduction of various amounts of gold precursors to poly((4-vinylpyridine)-block-(ε-caprolactone) (P4VP-b-PCL) diblock copolymers [10]. Recently Kim and coworkers have demonstrated that block copolymer micelles (polystyrene-b-poly(acrylic acid) (PS-b-PAA)) in thin films can effectively act as template to produce well controlled nanocomposites with various structures through complexation with inorganic precursors and solvent annealing [11]. In this case, however, the reduction of inorganic precursors can sometimes destroy the dispersion of inorganic materials in the matrix, and it becomes difficult to control the size and shape of nanomaterials in the matrix.

Semifluorinated block copolymers are amphiphilic materials that combine the unique self-assembly characteristics of block copolymers and the unparalleled properties of fluorinated polymers. Fluorinated blocks have attracted much attention due to their unique properties such as low surface energy, excellent chemical and thermal stability, low refractive index and dielectric constant, chemical/biological inertness, and oil/water repellence, which cannot be achieved by the corresponding non-fluorinated materials [15-17]. Although a variety of methods have been developed to selectively incorporate nanoparticles into desired block copolymer domains, only few articles have been reported for the sintering of gold nanopartices through phase transition of BCP thin films.

This paper reports a simple *in situ* synthesis of gold nanoparticles in semifluorinated block copolymer thin films and size change of the nanoparticles through a phase transition of the BCP thin films. Three different annealing modes of $LiAuCl_4$-load block copolymeric thin films were employed: in solvent vapor annealing at 70 ^{0}C, in supercritical CO_2 at

70 ^{0}C and in a vacuum oven at 100 ^{0}C. $LiAuCl_4$, gold precursor complexed with BCP consisting of semifluorinated and PEO blocks were reduced to Au nanoparticles that were well dispersed in the PEO phase of the disordered BCPs micellar thin films. The same sample after annealing, the formation of larger single gold particle per PEO domain with a small variation in size was observed. Figure 2.1 shows a schematic diagram of the process.

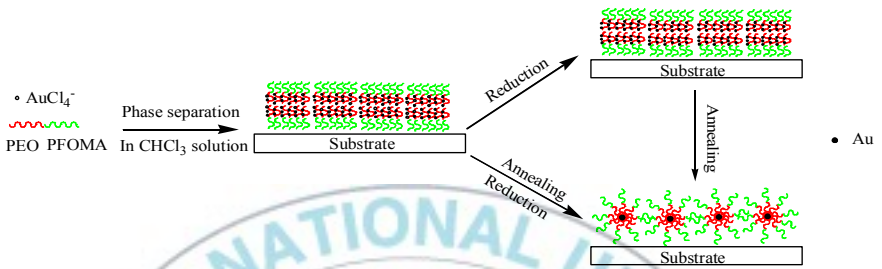

Figure 2.1. Schematic diagram of the assembly process for gold nanoparticles.

2.2. EXPERIMENT SECTION

2.2.1. Synthesis of block copolymers by ATRP

The semifluorinated diblock copolymers poly(ethylene oxide)-*b*-poly(1H,1H-dihydroperfluorooctyl methacrylate) (PEO-*b*-PFOMA) were synthesized by atom transfer radical polymerization (ATRP) of FOMA using PEO-Br as the macroinitiator in the mixed solvent of trifluorotoluene and benzene as described previously [18,19]. For this study, 10k was utilized to make PEO_{10k}-*b*-$PFOMA_{12k}$. The molecular structure of PEO-*b*-PFOMA is depicted in Figure 2.2.

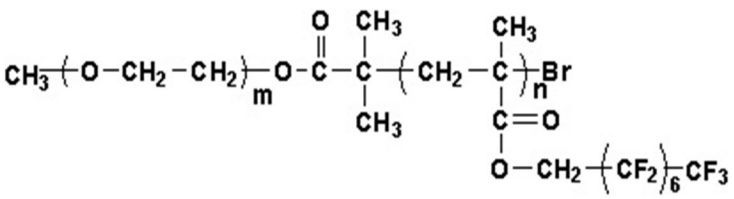

Figure 2.2. Molecular structure of PEO-*b*-PFOMA

2.2.2. Thin film preparation

PEO_{10k}-*b*-$PFOMA_{12k}$ was dissolved in chloroform to yield 0.5 wt% solutions. $LiAuCl_4$ loaded micellar solutions were prepared by adding 0.1 wt% of $LiAuCl_4$ (99.995%, Aldrich) into the pre-prepared copolymeric micellar solutions. The thin films were prepared on mica substrates by spin-coating of the BCPs micellar solutions and $LiAuCl_4$ treated micellar solutions. The prepared films were dried in the ambient atmosphere for 5 min.

2.2.3. Annealing

The micellar thin film was fabricated simply by spin-coating at 700 RPM from the chloroform solution of the block copolymer on a piece of freshly cleaved mica. The $LiAuCl_4$-loaded thin film on the mica was annealed in supercritical CO_2 in a high-pressure reactor. After charging the sample, the reactor was sealed and pressurized at 13.8 MPa with carbon dioxide (99.99 %) using a high-pressure syringe pump (ISCO-Model 2608) and the reactor was heated to 70 ^{0}C in a water bath for 24 h. The sample was taken for TEM analysis after depressurization by venting CO_2 from the top of the reactor. After annealing, the film was easily separated from the mica substrate by floating on water due to the strong affinity of water to mica. Such a film was transferable to a regular TEM copper grid having no supports. The $LiAuCl_4$-loaded thin film on mica substrate was also annealed in a vacuum oven at 100 ^{0}C for 24 h and examined with TEM analysis.

For solvent vapor annealing, the thin film was placed into a glass vessel with the reservoir of fluorinated solvent, PF-5080 (perfluoroalkanes, primarily compounds with 8 carbons). The temperature of the fluorinated solvent vapor was always kept at 70 ^{0}C. PEO-*b*-PFOMA films were exposed to solvent vapor to induce mobility and develop ordered nanostructures. After 12 h, the samples were taken out from the vessel and dried in the air at room temperature.

2.2.4. Characterization

^{1}H-NMR spectra of block copolymers were obtained in a mixed solvent of trichlorofluoromethane and $CDCl_3$ using a JNM-ECP 400 (JEOL). The composition of PEO_{10k}-*b*-$PFOMA_{12k}$ was determined by ^{1}H-NMR spectra,

from which the degree of polymerization was calculated. The morphologies of the thin films were investigated before and after annealing by transmission electron microscope (TEM) using a Hitachi H-7500 instrument operated at 80 kV.

2.3. RESULTS AND DISCUSSION

Amphiphilic block copolymers self-assemble into micelle-like objects when dissolved in solvents that are selective good solvents for one of the blocks. As previously reported, semifluorinated block copolymers with different block ratios give different micellar film morphologies [20,21]. The TEM image of as-spun asymmetric PEO_{10k}-*b*-$PFOMA_{12k}$ micellar films from chloroform (a good solvent for PEO chains) is shown in Figure 2.3a. The film was not subjected to any staining procedure due to the high electron density of PFOMA block [20]. The darker phase corresponds to the major component, the PFOMA blocks, and the lighter phase, comprising the minor component, the PEO blocks. When the soluble block is much shorter than the insoluble block, the aggregates form a crew-cut morphology. A variety of different morphologies can form for these types of polymers. One of the noteworthy phenomenon associated with crew-cut aggregates is the accessibility of a wide range of morphologies such as spheres, rods, vesicles, lamellae, a hexagonally packed hollow structure, large compound micelles and nanotubes [22]. It can be seen that the as-spun PEO_{10k}-*b*-$PFOMA_{12k}$ film showed a crew-cut aggregate of worm-like micelles, uniform in width with average sizes of 25 nm in PFOMA blocks, because the fraction of insoluble PFOMA blocks in the copolymers is larger than PEO blocks. $LiAuCl_4$ loaded micellar solutions were prepared by adding 0.1 wt % of $LiAuCl_4$ into the pre-prepared copolymeric micellar solutions. When the block copolymer solution was treated with solid $LiAuCl_4$, the salt was slowly solubilized as the Li^+ ions formed complexes with ethylene oxide units of the block copolymer and the tetrachloroaurate ions are bound as counter ions within the PEO phase of the micelles [23]. Figure 2.3b shows TEM images of the thin films spin-coated from the $LiAuCl_4$-loaded micellar solution of PEO-*b*-PFOMA. The gray regions are the PFOMA phase in

accordance with the higher electron density of the fluorinated blocks. The bright color of the PEO phase is marked by dark dots, which are gold nanoparticles resulting from the reduction of tetrachloroaurate ions due to an interaction with PEO chains [24].

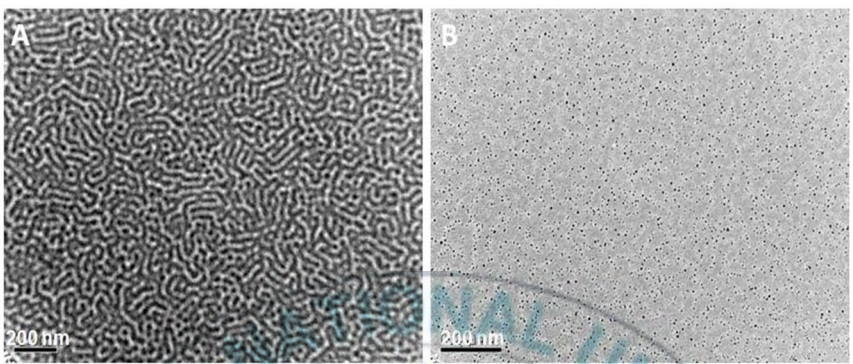

Figure 2.3. TEM image of (A) PEO-*b*-PFOMA micellar thin films and (B) gold nanoparticles produced in the micellar thin films of PEO-*b*-PFOMA, spin-cast from chloroform solutions at room temperature.

As shown in Figure 2.3b, it is clear that gold nanoparticles are well dispersed in the PEO phase and were not located in the entire PFOMA phase. And it showed a denser array of nanoparticles as our expectation. In the thin films, the average diameter of the gold nanoparticles was 6 nm. The effects of nanoparticles addition on the structure of block copolymers have been investigated by several groups [25-29]. Some have focused on the location of added nanoparticles within block copolymer domains [25,26], and others have observed the nanoparticle induced phase transition of block copolymers [27-29]. Recently, it was reported that the morphology in block copolymer films were varied in depth by adding high concentration of nanoparticles. However, such spatial variation of morphology was observed only for thick films, but not expected for thin films containing one or two layers of micelles [11], as in our case. Typical structure of micellar films is observed as in the case without Au precursors, showing nanoparticle-ineffective behavior over the block copolymer morphologies in our work.

For phase transition, the thin films were annealed under saturated PF-5080 at 70 ^{0}C, in a supercritical fluid ($scCO_2$) environment at 70 ^{0}C, or thermally at 100 ^{0}C in a vacuum oven (Figure 2.4). Each treatment imparts mobility to the BCP thin films, allowing them to reach the equilibrium morphology. Fluorine-containing polymers are highly solvophobic (lipo- and hydrophobic), i.e. they are insoluble in common organic solvents but are soluble in fluorinated solvents. This leads to easy phase-separation in BCP thin films as well as facile self assembly in organic sovents [16,17]. Figure 2.4a shows TEM image of the thin film spin-coated from the $LiAuCl_4$-loaded micellar solution of PEO-*b*-PFOMA. It shows the worm-like morphologies in which the gray regions are the PFOMA phase in accordance with the higher electron density of the fluorinated blocks, the bright color of the PEO phase is marked by dark dots. The TEM images in Figure 2.4b are shown the effects of solvent annealing for the micellar films of PEO-b-PFOMA complexed with Au precursors, where PF-5080 was used as a solvent for annealing at 70 ^{0}C. This temperature was chosen so that solvent vapor annealing was kept above the glass transition temperature (T_g) of the PEO and PFOMA, given complications that may arise from crystallization [30,31]. Solvent vapor annealing is a useful method for increasing domain size [32-35]. In this technique, the copolymer mobility is increased as the film absorbs solvent from the vapor phase. The plasticizing effect of the solvent reduces the glass transition temperature of the blocks below ambient temperature, allowing the copolymer nanostructure to relax into a lower energy, defect-free orientation [36-38]. During PF-5080 annealing, PFOMA block absorbed more PF-5080 than PEO due to the selective solvent of PF-5080 for PFOMA blocks. Hence, the mobility of PFOMA was larger than that of PEO. The smaller surface energy of PFOMA than PEO made PFOMA blocks tend to move towards the air surface. In addition, the attraction between PFOMA and PF-5080 was also favorable for PFOMA exposing to the air surface, the repulsion between the PEO and PF-5080 made PEO move towards the substrate. Based on these facts, there was more PFOMA located at the air surface after treatment, and the film exhibited spherical morphology of the PEO domain. During phase transition, the nanoparticles were moved together with the PEO blocks,

leading to the formation of a larger single particle in each domain. The average diameter of the gold nanoparticles was calculated to be 11 nm, respectively.

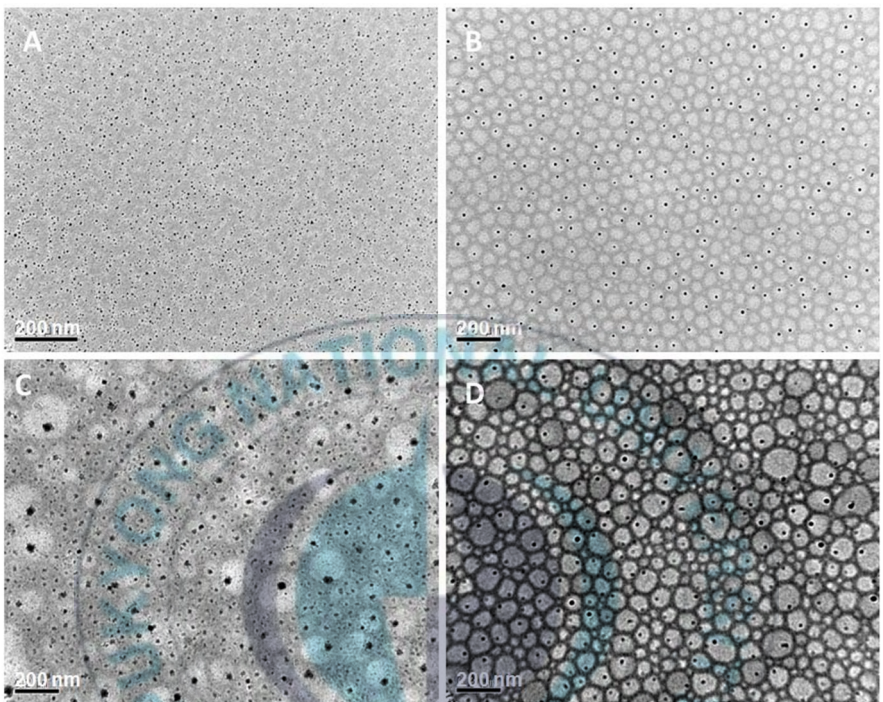

Figure 2.4. TEM images of gold nanoparticles produced in micellar thin films of PEO-*b*-PFOMA, (A) spin-cast film from chloroform solutions, (B) after PF-5080 solvent vapor treatment, (C) after annealing in $scCO_2$ and (D) after annealing in a vacuum oven.

The $LiAuCl_4$-loaded thin film samples were also annealed in supercritical CO_2 in a high-pressure reactor. A sample was taken for TEM analysis after depressurization by venting CO_2 from the top of the reactor. The presence of $scCO_2$ on the free surface of thin films can strongly influence the interfacial interactions, effectively modify the kinetics of phase segregation, and substantially affect the wetting behavior. $ScCO_2$ is a solvent for hydrophobic polymers such as fluorinated polymers [39-41], therefore, $scCO_2$ can penetrate into fluorinated block copolymers and swell the fluorinated blocks significantly. Figure 2.4c shows morphologies of

$LiAuCl_4$-load thin film samples after $scCO_2$ annealing. The strong affinity between PFOMA and CO_2 induced phase segregation when annealing PEO-b-PFOMA films at 70 ^{0}C. Upon desorption of CO_2, the diblock films rapidly cross the glass transition and become "frozen" [42]. The "frozen" PEO core would, therefore, have a size somewhere between the pure unswollen PEO and the CO_2 swollen PEO and reside on the substrate. The PFOMA block, owing to its substantially lower surface tension, resides on the free surface. In the annealing procedure, the nanoparticles were constrained to follow the continuous films and produced single large particles in the PEO domains. After annealing in $scCO_2$, the average diameter of the gold nanoparticles was calculated to be 19 nm, respectively.

Thermal annealing is performed by raising the temperature above the glass transition temperature of all the copolymer block, when the polymer chains have sufficient mobility to rearrange the film into the favored ordered state [43-45]. In order to determine if this hypothesis applies to Au-loaded BCP thin films, the films were subjected to thermal annealing at 100 ^{0}C in a vacuum oven for 24 h (the upper glass transition temperature of PFOMA is 45 ^{0}C). As shown in Figure 2.4d, the resulting morphologies were changed to spherical and the average diameter of the single gold nanoparticles embedded inside the PEO domains was 13 nm. The particle size distribution of the gold nanoparticles from annealing at 100 ^{0}C was smaller than that from annealing in $scCO_2$ at 70 ^{0}C but broader than that from annealing in PF-5080 vapor at 70 ^{0}C. In the case of PF-5080 vapor annealing, the micellar structure undergoes rapid transition in solvent environment that is highly selective toward fluorinated polymer chains. But in the case of $scCO_2$ annealing, many gold nanoparticles were observed. In fact, the solvent quality can be easily adjusted with pressure and temperature. Moreover, plasticization of the film and supercritical fluid absorption may also enhance diffusion of the nanoscopic particles in comparison to liquids solvents, facilitating the sintering of nanoparticles within the BCP. It is most likely that all nanoparticles locating in the PEO phase were constrained to follow the morphological change more easily than in the case of thermal and solvent treatment.

2.4. CONCLUSION

In conclusion, this study demonstrated the formation of larger single gold nanoparticles in each phase PEO domain from a number of well dispersed smaller gold nanoparticles within the self-assembled copolymeric thin films after annealing. PEO_{10k}-*b*-$PFOMA_{12k}$ diblock copolymers provide an excellent means of producing well dispersed gold nanoparticles in the PEO phase with an average particle diameter of 6 nm. Using selective solvent annealing as a means of controlling the size and location of the nanoparticles within the periodic structure of BCPs is feasible. While the phase transitions that enable control of the size and location of the nanoparticles within a bulk BCP can be accomplished by exposing a BCP to any selective solvent, the use of supercritical fluids offers the possibility of tuning the morphology of the polymer in a very controlled manner. Sintering of nanoparticles using phase transition of semifluorinated BCP is a simple and versatile method that can be extended to other particles.

3.5 REFERENCES

1. I. W. Hamley, *Angew. Chem., Int. Ed. 42*, 1692, 2003.
2. R. Shenhar, T. B. Norsten and V. M. Rotello, *Adv. Mater*. 17(6), 657, 2005.
3. T. F. Jaramillo, S. H. Baeck, B. R. Cuenya and E. W. McFarland, *J. Am. Chem. Soc.* 125, 7148, 2003.
4. W. A. Lopes and H. M. Jaeger, *Nature* 414, 735, 2001.
5. M. Haruta, *Catal. Today* 36 153, 1997.
6. J. J. Chiu, B. J. Kim, E. J. Kramer and D. J. Pine, *J. Am. Chem. Soc.* 127, 5036, 2005.
7. S. W. Yeh, K. H. Wei, Y. S. Sun, U. S. Jeng and K. S. Liang, *Macromolecules 38*, 6559, 2005.
8. L. Meli, Y. Li, K. T. Lim, K. P. Johnston and P. F. Green, *Macromolecules* 40, 6713, 2007.

9. B. H. Sohn, S. I. Yoo, B. W. Seo, S. H. Yun and S. M. Park, *J. Am. Chem. Soc. 123*, 12734, 2001.

10. R. M. Ho, T. Lin, M. R. Jhong, T. M. Chung, B. T. Ko and Y. C. Chen, *Macromolecules 38,* 8607, 2005.

11. A. J. Jang, L. Seung-kyu and S. H. Kim, *Polymer 51*, 3486-3492, 2010.

12. Y. Lin, A. Boker, J. He, K. Sill, H. Xiang, C. Abetz, X. Li, J. Wang, T. Emrick, S. Long, Q. Wang, A. Balazs and T. P. Russell, *Nauture* 434, 55, 2005.

13. J. Dockendorff, M. Gauthier, A. Mourran, M. Moller, *Macromolecules* 41, 6621, 2008.

14. M. Aizawa, J. M. Buriak, *Chem Mater.* 19, 5090, 2007.

15. Z. B. Zhang, S. K. Yinga, Z. Q. Shi, *Polymer* 40, 5439, 1999.

16. T. Imae, *Current Opinion in Colloid and Interface Science* 8, 307, 2003.

17. A. Hirao, K. Sugiyama and H. Yokoyama, *Prog. Polym. Sci. 32,* 1393, 2007.

18. K. T. Lim, M. Y. Lee, M. J. Moon, G. D. Lee, S. S. Hong, J. L. Dickson and K. P. Johnston, *Polymer* 43, 7043, 2002.

19. H. S. Hwang, J. Y. Heo, Y. T. Jeong, S. H. Jin, D. Cho, T. Chang and K. T. Lim, *Polymer* 44, 5153, 2003.

20. M. Y. Lee, S. H. Kim, J. T. Kim, S. W. Kim and K. T. Lim, *J. Nanosci. Nanotechnol. 8*, 4864, 2008.

21. M. Y. Lee, C. Park, S. S. Hong, Y. S. Gal and K. T. Lim, *Solid State Phenom. 425*, 121, 2007.

22. L. Zhang and A. Eisenberg, *J. Am. Chem. Soc. 118*, 3168, 1996.

23. J. P. Spatz, A. Roescher and M. Moller, *Adv. Mater. 8*, 337, 1996.

24. T. Sakai and P. Alexandridis, *J. Phys. Chem. B 109*, 7766, 2005.

25. J. J. Chiu, B. J. Kim, E. J. Kramer and D. J. Pine, *J. Am. Chem. Soc.* 127 (14), 5036-5037, 2005.

26. M. R. Bockstaller, Y. Lapetnikov, S. Margel and E. L. Thomas, *J. Am. Chem. Soc.* 125, 5276-5277, 2003.

27. J. Huh, V. V. Ginzburg, A. C. Balazs, *Macromolecules* 33 (21), 8085-8096, 2000.

28. B. J. Kim, J. J. Chiu, G. R. Yi, D. J. Pine and E. J. Kramer, *Adv. Mater.* 17, 2618-2622, 2005.

29. M. W. Matsen, R. B. Thompson, *Macromolecules* 41(5), 1853-1860, 2008.

30. L. A. Madsen, *Macromelecules* 39, 1483, 2006.

31. Y. Li, X. Wang, I. C. Sanchez, K. P. Johnston and P. F. Green, *J. Phys. Chem. B 111*, 16-25, 2007.

32. G. Kim, M. Libera, *Macromolecules* 31, 2569, 1998.

33. H. Y. Huang, F. J. Zhang, Z. J. Hu, B. Y. Du, T. B. He, F. K. Lee, Y. J. Wang and O. K. C. Tsui, *Macromolecules* 36, 4084, 2003.

34. K. Fukunaga, T. Hashimoto, H. Elbs and G. Krausch, *Macromolecules* 35, 4406, 2002.

35. H. Elbs, C. Drummer, V. Abetz and G. Krausch, M*acromolecules* 35, 5570, 2002.

36. J. Peng, D.H. Kim, W. Knoll, Y. Xuan, B. Y. Li and Y. C. Han, *J. Chem. Phys.* 125, 064702, 2006.

37. S. H. Kim, M. J. Misner and T. P. Russell, *Adv Mater* 16, 2119, 2004.

38. K. Fukunaga, H. Elbs, R. Magerle and G. Krausch, *Macromolecules* 33, 947, 2000.

39. R. Triolo, A. Triolo, F. Triolo, D. C. Steytler, C. A. Lewis, R. K. Heenan, G. D. Wignall and D. Simone, *J. M. Phys. Rev. E*, *61,* 4640, 2000.

40. M. L. O'Neill, Q. Cao, M. Fang and K. P. Johnston, *Ind. Eng. Chem. Res. 37,* 3067-3079, 1998.

41. H. Yokoyama and K. Sugiyama, *Langmuir 20,* 10001-10006, 2004.

42. Y. Li, L. Meli, K. T. Lim, K. P. Johnston and P. F. Green, *Macromolecules 39,* 7044-7054, 2006.

43. K. S. Iyer, J. Moreland, I. Luzinov, S. Malynych and G. Chumanov, *ACS Symposium Series*, Vol. 941, 2006.

44. R. O. Valles, S. Guo, M. S. Lund, C. Leighton and M. A. Hillmyer, *Macromolecules*, 38 (24), 10101-10108, 2005.

45. R. J. Albalak and E. L. Thomas, *Polymer,* Vol. 38, No. 15, 3819-3825, 1997.

Chapter 3

GOLD/SEMI-FLUORINATED BLOCK COPOLYMER NANOCOMPOSITES DEVELOPED IN THIN FILM WITH ANNEALING

Herein, an approach for preparing the ordered structures of Au/polymer nanocomposites is discussed, which employs solvent vapor, supercritical CO_2 and thermal annealing process for Au-loaded poly(3-hexyl thiophene)-block-poly(1H,1H-perfluorooctyl methacrylate) (P3HT-b-PFOMA) thin films. The block copolymers underwent microphase separation and self-assembly into well-defined and organized nanofibrillar-like morphology from their micelle solution. The gold nanoparticles were stabilized by the interaction of the sulfur atoms of P3HTs with the gold surface and they dispersed in the P3HT phase. The length of nanofibrils increased a little with pronounced branching after thermal annealing, solvent annealing and $scCO_2$ annealing in the micellar films with the Au nanoparticles.

3.1. INTRODUCTION

Regioregular poly(3-alkylthiophenes) (PATs) belong to a class of conjugated polymers that are highly conductive in their oxidized state, yet soluble and environmentally stable [1,2]. These properties enable PATs to be significantly useful in a wide variety of applications ranging from chemical and optical sensors, smart windows, light emitting diodes, displays and memory devices [1,3]. In particular, poly(3-hexylthiophene) (P3HT) has proven its usefulness in organic field effect transistors [4], and has shown the highest performances in organic solar cell devices [5].

The self-assembly of block copolymers into a nanostructure with novel morphology and property has attracted an increasing interest as a new approach for materials science, chemical synthesis, and nanofabrication [6,7]. Most theoretical and experimental studies have concentrated on the assembly characteristics of coil-coil block copolymers. Recently, rod-coil block copolymers have received a great deal of attention since they offer an attractive strategy for the organization of many highly functional rod-like polymers such as helical biopolymers and conducting polymers with rigid π-conjugated backbones [7-11]. In particular, block copolymers containing conducting polymer segments, such as polyfluorene, poly(phenylene vinylene), have received much attention because of their prompt application to a wide variety of optoelectric devices. On the other hand, fluorinated block copolymers are of growing interest due to their unique properties such as low surface energy, excellent chemical and thermal stability, low refractive index and dielectric constant, chemical/biological inertness, and oil/water repellence, which cannot be achieved by corresponding non-fluorinated materials [12-15]. These unique properties of semifluorinated blocks may be transferred to other polymeric materials by copolymerization. The modification of some characteristics of polymeric materials by the addition of semifluorinated blocks represents a goal of increasing importance. The unique behavior resulting from the dissimilar blocks, thus drives a self-assembly by polymer phase separation.

Polymeric nanocomposites are commonly defined as a binary mixture of functional inorganic nanomaterials dispersed in a polymeric matrix. The

stabilization of nanoparticles (NPs) with polymers has been investigated by a number of groups [16,17]. Although innumerable research articles were shown in the literature for the self-assembly of BCPs and the morphological development of the hybrid films of BCPs and NPs [18-20], few works have been reported for the block copolymers of π-conjugated and fluorinated polymers which have potential applications to optical and microelectonics devices. In this work, semifluorinated BCP micelles are used as a template for composites to generate well-dispersed NPs with uniform size and shape without severe aggregation. Three different annealing modes of Au-loaded block copolymeric thin films were employed: in solvent vapor, in supercritical CO_2 at 70 ^{0}C and in a vacuum oven at 150 ^{0}C.

3.2. EXPERIMENT SECTION

3.2.1. Synthesis of block copolymers by ATRP

The semifluorinated diblock copolymers poly(3-hexylthiophene)-b-poly(1H, 1H-dihydroperfluorooctyl methacrylate) (P3HT-b-PFOMA) were synthesized by atom transfer radical polymerization (ATRP) of FOMA using P3HT-Br as the macroinitiator in the mixed solvent of toluene and trifluorotoluene as described previously [21]. The molecular structure of P3HT-b-PFOMA is depicted in Figure 3.1.

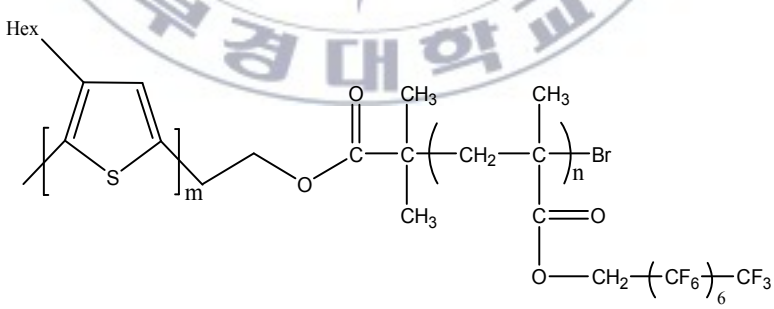

Figure 3.1. Molecular structure of P3HT-b-PFOMA

3.2.2. In-situ synthesis of gold nanoparticles and ordering of the prepared micellar thin film

The micellar thin film was fabricated by spin-coating at 700 RPM from the chloroform solution (1 wt%) of the BCP on a piece of freshly cleaved mica. The $LiAuCl_4$-loaded micellar solutions were prepared by adding 0.1 wt% of $LiAuCl_4$ into the pre-prepared copolymeric micallar solutions. The $LiAuCl_4$-loaded thin film on the mica was annealed in $scCO_2$ in a high-pressure reactor. After charging the sample, the reactor was sealed and pressurized at 13.8 MPa with carbon dioxide using a high-pressure syringe pump (ISCO-Model 2608) and the reactor was heated to 70 ^{0}C in a water bath for 12 h. The sample was taken for TEM analysis after depressurization by venting CO_2 from the top of the reactor. After annealing, the film was easily separated from the mica substrate by floating on water due to the strong affinity of water to mica. The film was transferred to a regular TEM copper grid having no supports. The $LiAuCl_4$-loaded thin film on mica substrate was also annealed in a vacuum oven at 150 ^{0}C for 24 h and examined with TEM analysis.

For solvent vapor annealing, the thin film with gold or without gold was placed into a glass vessel with the reservoir of a fluorinated solvent, perfluoroalkanes - primarily compounds with 8 carbons (PF-5080) or triflurotoluene (TFT). The temperature of the fluorinated solvent vapor was always kept at 70 ^{0}C. P3HT-*b*-PFOMA films were exposed to different solvent vapors for different periods to induce mobility and develop ordered nanostructures. After the vapor treatment, the samples were taken out from the vessel and dried in the air at room temperature.

3.2.3. Characterization

^{1}H NMR spectra were obtained in $CDCl_3$ and a mixed solvent of trichlorofluoromethane and $CDCl_3$ for the P3HT macroinitiator and the semifluorinated block copolymers, respectively using a JNM-ECP 400 (JEOL). The morphologies of the thin films were investigated by transmission electron microscope (TEM) using a Hitachi H-7500 instrument operated at 80 kV.

3.3. RESULTS AND DISCUSSION

3.3.1. TEM studies of nanostructered morphology

A new type of π-conjugated block copolymer of semifluorinated poly(fluorooctyl methacrylate) was synthesized by ATRP. ATRP yielded diblock copolymers with well-defined molecular weights. The second block, poly(fluorooctyl methacrylate) (PFOMA) is a semifluorinated polymer with several interesting properties of its own [22-25]. For this study, 4k of P3HT was used as macroinitiator to produce $P3HT_{4k}$-b-$PFOMA_{14k}$. Rod-coil diblock copolymers containing P3HT can have good electrical properties despite the presence of the insulating segment, because they self-assemble into long conductive nanofibrils that provide paths for charges between electrodes. Nano-ordered microphase separation has been found in a rod-coil block copolymer film, similar to a conventional coil-coil block copolymer, induced by spontaneous self-assembly of each immiscible segment in which domains rich in one block are separated from domains rich in the other so as to minimize contact energy. In our work, the nanoscale morphology of the BCP in the solid-state was investigated using TEM for films cast from chloroform. Regioregular poly(3-hexylthiophene) forms a characteristic nanofibrillar morphology. TEM image of P3HT-b-PFOMA copolymer is shown in Figure 3.2A, where nanofibrillar morphology is clearly evident, pointing to the prevalence of this type of supramolecular structure in P3HT based materials [26-28]. A control experiment was performed in order to assign the specific phases in the TEM image to P3HT and PFOMA blocks of the copolymer. The Figure 3.2B shows the TEM image of as-spun asymmetric $P3HT_{4k}$-b-$PFOMA_{14k}$ micellar films from chloroform after adding 50 wt% of the PFOMA homopolymer. It can be seen that the nanofibrils were changed to the densely packed shape with the addition of the PFOMA homopolymer into the block copolymer. Therefore, it is considered that the darker phase and lighter phase in the TEM images correspond to the major component, the PFOMA blocks and the minor component, the P3HT blocks, respectively. The electron density of semifluorinated PFOMA blocks could be higher than P3HT. The obtained nanofibrillar microstructure is the result of

interplay between different driving forces of self-assembly (π-stacking versus phase separation).

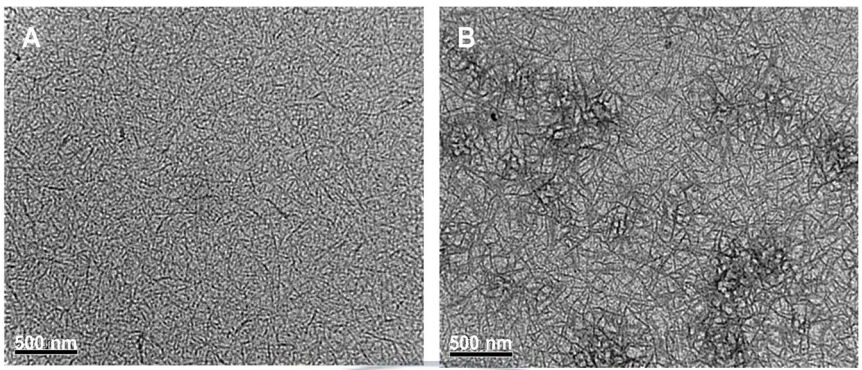

Figure 3.2. TEM images of the self-assembled structure of P3HT-*b*-PFOMA copolymeric thin films: (A) spin cast thin film, and (B) after adding PFOMA homopolymer (50%).

The development of the surface morphology of P3HT-*b*-PFOMA copolymeric thin films was further investigated with annealing in PF-5080 and TFT solvent vapor, which are selective solvents for the PFOMA block,. When the samples are exposed to solvent vapor at 70 ^{0}C, the mobility is imparted to the system, as when the polymer is heated above its transition glass temperature (T_g), and the morphology would change. Therefore, it is interesting to investigate the process of morphology evolution under various solvent vapors. During fluorinated solvent annealing, the PFOMA block absorbed more PF-5080 than P3HT due to the selective solubility of PF-5080 for PFOMA blocks. Hence, the mobility of PFOMA was larger than that of P3HT. The morphologies of polymer films with the same thickness (approximately 80 nm) but different annealing times were investigated (Figure 3.3).

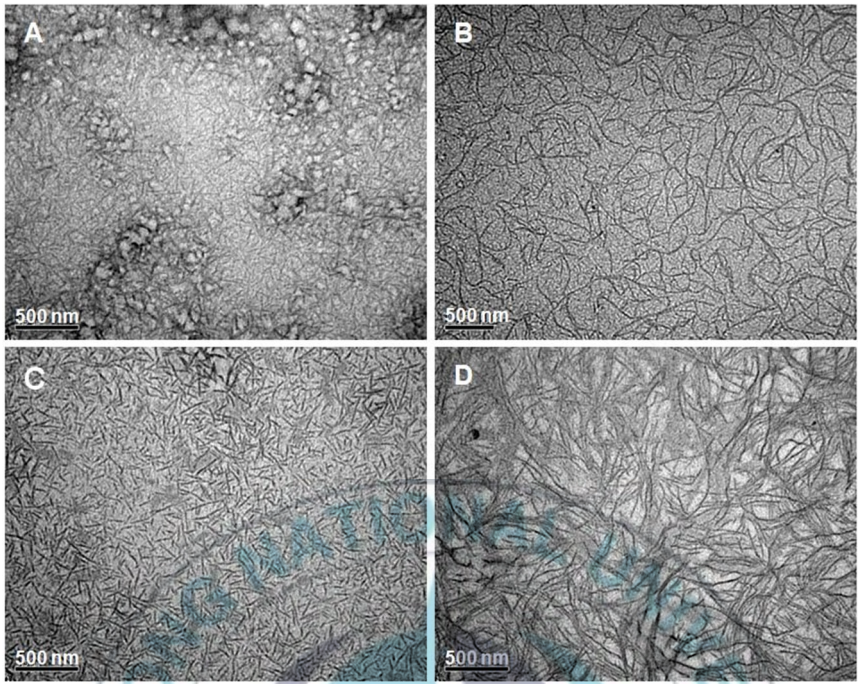

Figure 3.3. TEM micrographs of $P3HT_{4k}$-b-$PFOMA_{14k}$ thin films prepared from 1 wt% solutions of BCP in chloroform, obtained after PF-5080 vapor annealing for (A) 4 h and (B) 16 h, and TFT vapor annealing for (C) 4 h and (D) 16 h.

After 4 h, the film displayed a featureless morphology, just like the as-cast film after PF-5080 vapor annealing as shown in Figure 3.3A. An incomplete change was also observed in this morphology, indicating the PF-5080 vapor treatment for 4 h is not enough to reach in an equilibrium morphological state. However, upon longer annealing, P3HT nanofibrils and dark PFOMA aggregates are well developed. The morphology was developed to the dendrimer structure with longer nanofibrils after annealing in PF-5080 for 16 h (Figure 3.3B). The as-cast thin film was also subjected to the TFT solvent vapor annealing. The development of the morphology of the micellar thin films in TFT vapor which has also preferential affinity for PFOMA blocks was investigated by TEM. After annealing in TFT solvent vapor environment for 4 h, no specific morphology was formed as shown in Figure 3.3C. After 16 h of TFT vapor annealing, nanofibrillar morphology

of $P3HT_{4k}$-b-$PFOMA_{14k}$ was distinctly different (Figure 3.3D). The nanofibrils were longer than that from PF-5080, isolated from one another, and were randomly oriented throughout the sample. All the branched longer nanofirillar domains eventually form a networked morphology after annealing in TFT solvent vapor for 16 h. The formation of nanofibrillar structure of P3HT-b-PFOMA copolymers is undoubtedly dictated by the phase separation and crystallization of P3HT blocks [29,30]. The formation of quasi-one-dimensional objects such as nanofibrils indicates that the block copolymer self-assembles in a highly anisotropic way. Moreover, the phase separation between P3HT and PFOMA chains most probably takes place within nanoscale structure because P3HT and PFOMA segments are highly immiscible. The final nanofibrillar morphology must therefore be a compromise between the molecular organizations typical of each subphase.

3.3.2. Ordering of gold nanoparticles in nanodomains

For the preparation of ordered AuNP/polymer thin films, the copolymers were first dissolved in $CHCl_3$. The $LiAuCl_4$-loaded micellar solution were prepared by adding 0.1 wt% of $LiAuCl_4$ into the pre-prepared copolymeric micellar solutions. A freshly prepared aqueous solution of sodium borohydride was added slowly to the mixture with vigorous stirring. The color change from orange to dark purple evidenced the formation of AuNPs and the interaction with metal ions by sulfur atoms of P3HT. Torsi *et al.* has shown that conjugated polymers can stabilize inorganic nanoparticles by coordinating or forming complexes with the inorganic nanoparticles [31]. Furthermore, Ng *et al.* has demonstrated that sulfur atoms of polythiophenes can interact with metal ions [32]. Hence, it is assumed that the AuNPs are stabilized by the interaction of the sulfur atoms of poly(3-hexylthiophene)s with the gold surface. Figure 3.4A shows the TEM image of the thin film spin-coated from the $LiAuCl_4$-loaded micellar solution of P3HT-b-PFOMA. It shows the nanowire morphologies in which the gray regions are the PFOMA phase in accordance with the higher electron density of the fluorinated blocks, the bright color of the P3HT phase is marked by dark dots which are gold nanoparticles resulting from the reduction of tetrachloroaurate. It is notable that the morphology of the micelles with NPs

is similar to the micelles without the particles, from previous images (Figure 3.2A). In the thin film, the average diameter of the AuNPs was calculated to be 8 nm.

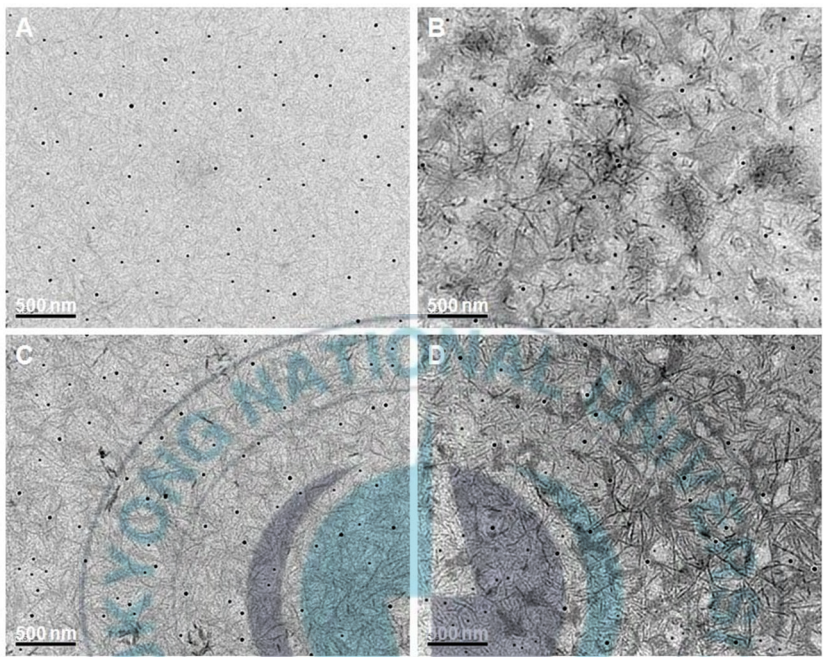

Figure 3.4. TEM images of gold nanoparticles produced in micellar thin films of P3HT-*b*-PFOMA: (A) spin-cast film from chloroform solutions, (B) after annealing in a vacuum oven at 150 ^{0}C, (C) after PF-5080 solvent vapor treatment at 70 ^{0}C and (D) after annealing in scCO_2 at 70 ^{0}C.

For phase develpment, the thin films were attempted to anneal under saturated PF-5080 at 70 ^{0}C, in a supercritical CO_2 environment at 70 ^{0}C, or thermally at 150 ^{0}C in a vacuum oven (Figure 3.4). Each treatment imparts mobility to the BCP thin films, allowing them to reach their equilibrium morphology. The upper glass transition temperature of PFOMA is 58 ^{0}C. The high temperature provides sufficient thermal energy for the chains to reorganize as they try to reach thermodynamic equilibrium. Fluorine-containing polymers are highly solvophobic (lipo- and hydrophobic), i.e. they are insoluble in common organic solvents but are soluble in fluorinated solvents. This leads to easy phase-separation in BCP thin films as well as

facile self assembly in organic solvents [33]. We also examined the morphological structures of the Au-loaded thin films upon annealing in $scCO_2$. Due to its high diffusivity and solubility for fluorous polymers, it has been reported that $scCO_2$ annealing accelerates the ordering process of the block copolymers [34]. $ScCO_2$ can penetrate into fluorinated block copolymers and swell the fluorinated blocks selectively. All the experimental results shows branched, and eventually connected to other nanofibrils after the annealing. The length of the nanofibrils increased a little with pronounced branching. The gold nanoparticles were produced in the thin films of P3HT-b-PFOMA and dispersed in the P3HT phase. In the thin films, the average diameter of the gold nanoparticles was in the range of 9-11 nm after annealing.

3.4. CONCLUSION

π-Conjugated and semifluorinated diblock copolymers consisting of P3HT and PFOMA were synthesized by ATRP using the end functionalized P3HT as the macroinitiator. The diblock copolymers exhibited a range of densely packed nanofibrillar morphologies with variable degrees of interfibrillar order. The ordering is improved by solvent vapor annealing under PF-5080 and TFT, where the block copolymeric thin films show nanometer-scale nanofibrillar morphologies. It was also demonstrated that BCP micelles in thin films effectively act as a template to produce nanocomposites through complexation with gold precursors and annealing. The gold nanoparticles are stabilized by the interaction of the sulfur atoms of P3HTs with the gold surface and it dispersed in the P3HT phase. The length of nanofibrils increased a little with pronounced branching after thermal annealing, solvent annealing and $scCO_2$ annealing of the micellar films with Au NPs. Regioregular poly(3-hexylthiophene)/gold nanoparticle hybrid materials may find applications in single-electron tunneling studies as well as organic field effect transistor.

3.5. REFERNCES

1. R. D. McCullough and P. C. Ewbank, ‘‘*Handbook of Conducting Polymers*’’ 2nd Edition, T. Skotheim, J. Reynolds, R. Elsenbaumer, Eds., Marcel Dekker, Inc., New York, 225, 1998.

2. M. C. Iovu, M. Jeffries-EL, E. E. Sheina, J. R. Cooper and R. D. McCullough, “Regioregular poly(3-alkylthiophene) Conducting Block Copolymers,” *Polymer* 46, 19, pp 8582-8586, 2005.

3. R. D. McCullough, “The Chemistry of Conducting Polythiophenes,” *Adv. Mater*. 10, pp 93-116, 1998.

4. Z. Bao and J. Locklin, ‘‘*Organic Field-Effect Transistors,*’’ 1st Edition, CRC Press, Boca Raton , 2007.

5. C. Brabec, V. Dyakonov and U. Scherf, ‘‘Organic Photovoltaics: Materials, Device Physics, and Manufacturing Technologies,’’ *Wiley-VCH, Weinheim*, 2008.

6. S. A. Jenekhe and X. L. Chen, “Self-Assembled Aggregates of Rod-Coil Block Copolymers and Their Solubilization and Encapsulation of Fullerenes,” *Science*, Vol. 279, No. 5358, pp 1903-1907, 1998.

7. H. A. Klok and S. Lecommandoux, “Supramolecular Materials via Block Copolymer Self-Assembly,” *Adv. Mater. 13*, pp 1217-1229, 2001.

8. W. J. Li, T. Maddux and L. P. Yu, “Synthesis and Characterization of Diblock Copolymers Containing Oligothiophenes with Defined Regiospecificity and Molecular Weights,” *Macromolecules 29*, pp 7329-7344, 1996.

9. K. Loos and A. H. E. Muller, “New Routes to the Synthesis of Amylose-*block*-polystyrene Rod-Coil Block Copolymers,” *Biomacromolecules 3*, pp 368-373, 2002.

10. M. S. Rahman, S. Samal and J. S. Lee, “Synthesis and Self-Assembly Studies of Amphiphilic Poly(*n*-hexylisocyanate)-*block*-poly(2-vinylpyridine)-*block*-poly(*n*-hexyl isocyanate) Rod-Coil-Rod Triblock Copolymer,” *Macromolecules 39*, pp 5009-5014, 2006.

11. V. Pryamitsyn and V. Ganesan, “Self-Assembly of Rod-Coil Block Copolymers,” *J. Chem. Phys. 120*, pp 5824-5838, 2004.

12. J. L. Kendall, D. A. Canelas, J. L.Young, and J. M. DeSimone, "Polymerizations in supercritical carbon dioxide," *Chem. Rev.* 99(2), pp 543-563, 1999.

13. J. G. Riess, "Fluorous micro- and nanophases with a biomedical perspective," *Tetrahedron* 58, pp 4113-4131, 2002.

14. V. V. Volkov, A. G. Fadeer, N. A. Plate, N. Amaya, Y. Murata, A. Takahara, and T. Kajiyama, "Effect of thermal molecular motion on pervaporation behavior of comb-shaped polymers with fluorocarbon side groups," *Polym. Bull*., Vol. 32, No. 2, pp 193-200, 1994.

15. I. Verweire, E. Schacht, B. P. Qiang, K. Wang, and I. Scheerder, "Evaluation of fluorinated polymers as coronary stent coating," *J. Mater. Sci. Mater. Med.* 11, pp 207-212, 2000.

16. C. H. Walker, J. V. St. John and P. Wisian-Neilson, "Synthesis and Size Control of Gold Nanoparticles Stabilized by Poly(methylphenylphosphazene)," *J. Am. Chem. Soc*. 123, pp 3846-3847, 2001.

17. M. A. Hempenius, B. M. W. Langeveld-Voss, J. A. E. H. Van Haare, R. A. J. Janssen, S. S. Sheiko, J. P. Spatz, M. Moller and E. W. Meijer, "A Polystyrene-Oligothiophene-Polystyrene Triblock Copolymer," *J. Am. Chem. Soc*. 120, pp 2798-2804, 1998.

18. A. J. Jang, L. Seung-kyu and S. H. Kim, "Structure and phase transition in thin films of block copolymer micelles complexed with inorganic precursors," *Polymer 51*, pp 3486-3492, 2010.

19. L. Meli, Y. Li, K. T. Lim, K. P. Johnston and P. F. Green, "Templating of gold nanocrystals in micellar cores of block copolymer films," *Macromolecules 40*, pp 6713-6720, 2007.

20. Y. Lin, A. Boker, J. He, K. Sill, H. Xiang, C. Abetz, X. Li, J. Wang, T. Emrick, S. Long, Q. Wang, A. Balazs and T. P. Russell, "Self-directed assembly of nanoparticles/copolymer mixtures," *Nature* 434, pp 55-59, 2005.

21. R. Md. Harun-Or, S. Myungeun, S. Y. Kim, Y. S. Gal and K. T. Lim "Synthesis and Properties of Diblock Copolymers Containing Poly(3-

Hexylthiophene) and Poly(Fluorooctyl Methacrylate)", *J. Nanosci. Nanotechnol.*, Vol. 11, No. 2, pp 1696-1700, 2011 .

22. K. T. Lim, M. Y. Lee, M. J. Moon, G. D. Lee, S. S. Hong, J. L. Dickson, and K. P. Johnston, "Synthesis and properties of semifluorinated block copolymers containing poly(ethylene oxide) and poly(fluorooctyl methacrylates) via atom transfer radical polymerization," *Polymer* 43, pp 7043-7049, 2002.

23. M. Y. Lee, S. H. Kim, J. T. Kim, S. W. Kim, and K. T. Lim, "Ordering transitions of semifluorinated diblock copolymers," *J. Nanosci. Nanotechnol.* 8, pp 4864-4868, 2008.

24. H. S. Hwang, H. J. Kim, Y. T. Jeong, Y. S. Gal and K. T. Lim, "Synthesis and Properties of Semifluorinated Copolymers of Oligo(ethylene glycol) Methacrylate and 1*H*,1*H*,2*H*,2*H*-Perfluorooctyl Methacrylate", *Macromolecules*. 37, pp 9821-9825, 2004.

25. H. S. Hwang, J. Y. Heo, Y. T. Jeong, S. H. Jin, D. Cho, T. Chang and K. T. Lim, "Preparation and properties of semifluorinated block copolymers of 2-(dimethylamino)ethyl methacrylate and fluorooctyl methacrylates," *Polymer* 44, pp 5153-5158, 2003.

26. M. C. Iov, C. R. Craley, M. Jeffries-EL, A. B. Krankowski, R. Zhang, T. Kowalewski and R. D. McCullough "Conducting Regioregular Polythiophene Block Copolymer Nanofibrils Synthesized by Reversible Addition Fragmentation Chain Transfer Polymerization (RAFT) and Nitroxide Mediated Polymerization (NMP)" *Macromolecules* 40, pp. 4733-4735, 2007.

27. G. Sauve' and R. D. McCullough, "High Field-Effect Mobilities for Diblock Copolymers of Poly(3-hexylthiophene) and Poly(methyl acrylate)," *Adv. Mater*. 19, pp 1822-1825, 2007.

28. T. Higashihara and M. Ueda, "Synthesis and characterization of a novel coil-rod-coil triblock copolymers comprised of regioregular poly(3-hexylthiophene) and poly(methyl methacrylate) segments," *React. Funct. Polym*. 69, pp 457-462, 2009.

29. H. Yang, T. J. Shin, L. Yang, K. Cho, C. Y. Ryu, and Z. Bao, "Effect of mesoscale crystalline structure on the field-effect mobility of

regioregular poly(3-hexyl thiophene) in thin-film transistors,"*Adv. Funct. Mater.* 15(4), pp 671-676, 2005.

30. S. Hugger, R. Thomann, T. Heinzel and T. Thurn-Albrecht, "Semicrystalline morphology in thin films of poly(3-hexylthiophene)," *Colloid Polym. Sci.* 282, pp 932-938, 2004.

31. Scamaracio, V. Tsakova, L. Sabbatini and P. G. Zammbonin, "Electrosynthesis and analytical characterization of nanostructured cooper-polypyrrole thin films," J. Mater. Chem. 11, pp 1434-1440, 2001.

32. S. C. Ng, X. C. Zhou, Z. K. Chen, P. Miao, H. S. O. Chan, S. F. Y. Li and P. Fu, "Quartz Crystal Microbalance Sensor Deposited with Langmuir-Blodgett Films of Functionalized Polythiophenes and Application to Heavy Metal Ions Analysis," Langmuir 14, pp 1748-1752, 1998.

33. V. S. RamachandraRao, R. R. Gupta, T. P. Russell and J. J. Watkins, *Langmuir* 17, pp 4342-4346, 2001.

34. T. Imae, "Fluorinated polymers," *Current Opinion in Colloid and Interface Science* 8, pp 307-314, 2003.

ACKNOWLEDGEMENTS

It has been a great honor for me to work with and to be surrounded with great people in Image Science Laboratory. To all, I say Thank you from the bottom of my heart.

Special and sincere thanks to my supervisor Prof. Kwon Taek Lim for all his support, encouragement, guidance, patience and knowledge. Thank you for your trust, effort, time and for all the opportunities you gave me.

My acknowledgements also go to Prof. Yeon Tae Jeong and Prof. Kim Jong Tae for reviewing my dissertation and giving me valuable comments and suggestions. Also, I would like to make a special mention about all professors in the Department of Image Science System and Engineering for their teaching and guidance throughout the study period.

Apart from the science knowledge, the financial support also played an important role in my Master study. I would like to express my sincere gratitude to the Korea Research Foundation (KRF) and Brain Korea 21 (BK21) for financial support of this work.

I would like express my heartfelt thanks to Pukyong National University authorities and the members of the office of the international relations for their cooperation in every possible aspect.

I wish to thank all my laboratory co-workers in our research group and friends in the department for their love and support. I want to present my thanks to my senior, Dr. Min Young Lee, who imparted to me experience and care. I am also sincerely thankful to my colleagues, whom I enjoyed working with. We have much discussion on researches, experiments and projects. During the years of study, I developed chummy friendship with them.

Lastly, and most importantly, I would like to express my deepest gratitude to my family for all their love and encouragement. For my parents who raised me with a love of science and supported me in all my pursuits. They gave me strength to reach for the stars and chase my dreams. Without their support and encouragements, I would have struggled to find the inspiration and motivation needed to complete this dissertation.

PUBLICATIONS

1. Nguyen Thi Hoai An and Kwon Taek Lim, **"Gold/Semi-fluorinated Block Copolymer Nanocomposites Developed in Thin Film with Annealing,"** Submitted to The Eighteenth International Conference on Composite Materials.

2. Nguyen Thi Hoai An and Kwon Taek Lim, **"Sintering of Nanoparticles Through Phase Transition of Block Copolymeric Micellar Thin Films,"** (Manuscript in preparation).